Kosho T, Miyake N, Hatamochi A, Takahashi J, Kato H, Miyahara T, Igawa Y, Yasui H, Ishida T, Ono K, Kosuda T, Inoue A, Kohyama M, Hattori T, Ohashi H, Nishimura G, Kawamura R, Wakui K, Fukushima Y, Matsumoto N.	A new Ehlers-Danlos syndrome with craniofacial characteristics, multiple congenital contractures, progressive joint and skin laxity, and multisystem fragility-related manifestations.	Am J Med Genet A.	31	284-294	2010
Miyake N, Kosho T, Mizumoto S, Furuichi T, Hatamochi A, Nagashima Y, Arai E, Takahashi K, Kawamura R, Wakui K, Takahashi J, Kato H, Yasui H, Ishida T, Ohashi H, Nishimura G, Shiina M, Saitsu H, Tsurusaki Y, Doi H, Fukushima Y, Ikegawa S, Yamada S, Sugahara K, Matsumoto N.	Loss-of-function mutations of CHST14 in a new type of Ehlers-Danlos syndrome.	Hum Mutat.	31	966-974	2010
Suzuki Y, Kure S, Oota M, Fukuda M	Nonketotic Hyperglycinemia: Proposal of a Diagnostic and Treatment Strategy.	Pediatr Neurol	43	221-224	2010
Kamada F, Aoki Y, Narisawa A, Abe Y, Komatsuzaki S, Kikuchi A, Kanno J, Niihori T, Ono M, Ishii N, Owada Y, Fujimura M, Mashimo Y, Suzuki Y, Hata A, Tsuchiya S, Tominaga T, Matsubara Y, Kure S	A genome-wide association study identifies RNF213 as the first Moyamoya disease gene.	J Hum Genet	56	34-40	2011

（作成上の留意事項）
1．「研究成果の刊行に関する一覧表」に記入した書籍又は雑誌は、その刊行物又は別刷り一部を添付すること。

2．研究報告書（当該報告書に含まれる文献等を含む。以下本留意事項において同じ。）は、国立国会図書館及び厚生労働省図書館並びに国立保健医療科学院ホームページにおいて公表されるものであること。研究者等は当該報告書を提出した時点で、公表について承諾したものとすること。
3．日本工業規格A列４番の用紙を用いること。各項目の記入量に応じて、適宜、欄を引き伸ばして差し支えない。

Ⅳ. 研究成果の刊行物・別刷

Journal of Human Genetics (2010) 55, 801–809

www.nature.com/jhg

ORIGINAL ARTICLE

Mutation analysis of the *SHOC2* gene in Noonan-like syndrome and in hematologic malignancies

Shoko Komatsuzaki[1], Yoko Aoki[1], Tetsuya Niihori[1], Nobuhiko Okamoto[2], Raoul CM Hennekam[3,4], Saskia Hopman[5], Hirofumi Ohashi[6], Seiji Mizuno[7], Yoriko Watanabe[8], Hotaka Kamasaki[9], Ikuko Kondo[10], Nobuko Moriyama[11], Kenji Kurosawa[12], Hiroshi Kawame[13], Ryuhei Okuyama[14], Masue Imaizumi[15], Takeshi Rikiishi[16], Shigeru Tsuchiya[16], Shigeo Kure[1,16] and Yoichi Matsubara[1]

Noonan syndrome is an autosomal dominant disease characterized by dysmorphic features, webbed neck, cardiac anomalies, short stature and cryptorchidism. It shows phenotypic overlap with Costello syndrome and cardio-facio-cutaneous (CFC) syndrome. Noonan syndrome and related disorders are caused by germline mutations in genes encoding molecules in the RAS/MAPK pathway. Recently, a gain-of-function mutation in *SHOC2*, p.S2G, has been identified as causative for a type of Noonan-like syndrome characterized by the presence of loose anagen hair. In order to understand the contribution of *SHOC2* mutations to the clinical manifestations of Noonan syndrome and related disorders, we analyzed *SHOC2* in 92 patients with Noonan syndrome and related disorders who did not exhibit *PTPN11*, *KRAS*, *HRAS*, *BRAF*, *MAP2K1/2*, *SOS1* or *RAF1* mutations. We found the previously identified p.S2G mutation in eight of our patients. We developed a rapid detection system to identify the p.S2G mutation using melting curve analysis, which will be a useful tool to screen for the apparently common mutation. All the patients with the p.S2G mutation showed short stature, sparse hair and atopic skin. Six of the mutation-positive patients showed severe mental retardation and easily pluckable hair, and one showed leukocytosis. No *SHOC2* mutations were identified in leukemia cells from 82 leukemia patients. These results suggest that clinical manifestations in *SHOC2* mutation-positive patients partially overlap with those in patients with typical Noonan or CFC syndrome and show that easily pluckable/loose anagen hair is distinctive in *SHOC2* mutation-positive patients.
Journal of Human Genetics (2010) **55,** 801–809; doi:10.1038/jhg.2010.116; published online 30 September 2010

Keywords: cardio-facio-cutaneous syndrome; costello syndrome; hematologic malignancy; loose anagen hair; melting curve analysis; noonan syndrome

INTRODUCTION

Noonan syndrome (MIM 163950) is an autosomal dominant disorder characterized by short stature, webbed or short neck, characteristic features (hypertelorism, low-set ears and ptosis), pulmonary valve stenosis and hypertrophic cardiomyopathy.[1,2] Noonan syndrome is a heterogeneous disease and overlaps phenotypically with Costello syndrome (MIM 218040) and cardio-facio-cutaneous (CFC) syndrome (MIM 115150). Costello syndrome is characterized by mental retardation, distinctive facial features, neonatal feeding difficulties, curly hair, loose skin, and hypertrophic cardiomyopathy and carries an increased risk of malignancy.[3] CFC syndrome, on the other hand, is characterized by mental retardation, ectodermal abnormalities (sparse hair, hyperkeratotic skin and ichthyosis), distinctive facial features (high forehead, bitemporal constriction, hypoplastic supraorbital ridges, downslanting palpebral fissures and depressed nasal bridge) and congenital heart defects (pulmonic stenosis, atrial septal defect and hypertrophic cardiomyopathy).[4]

Recent studies have shown that all three of these disorders result from dysregulation of the RAS/MAPK cascade. It has been suggested that these syndromes be comprehensively termed the RAS/MAPK syndromes[5] or the neuro-cardio-facial-cutaneous syndrome.[6] Germline mutations in *PTPN11*, *KRAS*, *SOS1* and *RAF1* have been

[1]Department of Medical Genetics, Tohoku University School of Medicine, Sendai, Japan; [2]Department of Medical Genetics, Osaka Medical Center and Research Institute for Maternal and Child Health, Izumi, Osaka, Japan; [3]Clinical and Molecular Genetics Unit, Institute of Child Health, Great Ormond Street Hospital for Children, University College London, London, UK; [4]Department of Pediatrics, Academic Medical Center, University of Amsterdam, Amsterdam, The Netherlands; [5]Department of Pediatric Oncology, Emma Children's Hospital, Academic Medical Center, Amsterdam, The Netherlands; [6]Division of Medical Genetics, Saitama Children's Medical Center, Saitama, Japan; [7]Department of Pediatrics, Central Hospital, Aichi Human Service Center, Aichi, Japan; [8]Department of Pediatrics and Child Health, Kurume University School of Medicine, Kurume, Japan; [9]Department of Pediatrics, Sapporo Medical University, Sapporo, Japan; [10]Division of Pediatrics, Oida Hospital, Kochi, Japan; [11]Department of Pediatrics, Hitachi Ltd, Mito General Hospital, Ibaraki, Japan; [12]Division of Medical Genetics, Kanagawa Children's Medical Center, Yokohama, Japan; [13]Department of Genetic Counseling, Ochanomizu University, Tokyo, Japan; [14]Department of Dermatology, Shinshu University School of Medicine, Matsumoto, Japan; [15]Department of Hematology and Oncology, Miyagi Children's Hospital, Sendai, Japan and [16]Department of Pediatrics, Tohoku University School of Medicine, Sendai, Japan
Correspondence: Dr Y Aoki, Department of Medical Genetics, Tohoku University School of Medicine, 1-1 Seiryo-machi, Sendai, Miyagi 980-8574, Japan.
E-mail: aokiy@med.tohoku.ac.jp
Received 14 June 2010; accepted 15 August 2010; published online 30 September 2010

identified in 60–80% of Noonan syndrome patients.[7–12] In patients with Costello syndrome, germline mutations in *HRAS* have been identified,[13] and mutations in *KRAS*, *BRAF* or *MAP2K1/MAP2K2* have been identified in approximately 70% of patients with CFC syndrome.[14,15] However, in approximately 40% of patients with these disorders, specific mutations have not been identified.

SHOC2 is homologous to *soc2*, a gene that was discovered in *Caenorhabditis elegans*. The *soc2* gene encodes leucine-rich repeats[16] and acts as a positive modulator of the RAS/MAPK pathway.[17] Recently, Cordeddu *et al.*[18] reported a gain-of-function missense mutation, c.4A>G (p.S2G), in *SHOC2* in patients with Noonan-like syndrome with loose anagen hair. However, clinical features of patients with a mutation in *SHOC2* remain unknown. In this study, we analyzed 92 patients with Noonan syndrome and related disorders to characterize mutations in the *SHOC2* gene. We also performed expression analysis of *SHOC2* in adult and fetal human tissues and performed sequence analysis of *SHOC2* in 82 leukemia samples.

MATERIALS AND METHODS

DNA samples from patients with Noonan syndrome and related disorders and from leukemia cells

We analyzed 92 patients with Noonan syndrome and related disorders who did not display *PTPN11*, *KRAS*, *HRAS*, *BRAF*, *MAP2K1/2* (*MEK1/2*), *SOS1* or *RAF1* mutations. At the time at which samples were sent, the primary diagnoses of these patients were as follows: 34 Noonan syndrome, 17 Costello syndrome, 21 CFC syndrome, 4 Noonan/CFC, 2 Costello/CFC and 14 others. Control DNA was obtained from 132 healthy Japanese individuals. Control DNA from 105 healthy Caucasian individuals was purchased from Coriell Cell Repositories (Camden, NJ, USA). Eighty-two leukemia DNA samples were collected from leukemia patients (32 acute myeloid leukemia, 41 acute lymphoblastic leukemia, 1 juvenile chronic myelogenous leukemia, 1 Ki-lymphoma, 2 malignant lymphoma, 1 myelodysplastic syndrome, 1 aplastic anemia, 2 transient abnormal myelopoiesis and 1 unknown). Nine additional genomic DNA samples were collected from patients who had developed leukemia and had achieved complete remission (eight acute lymphoblastic leukemia and one aplastic anemia).

This study was approved by the Ethics Committee of Tohoku University School of Medicine. We obtained informed consent from all subjects involved in the study and specific consent for photographs from seven patients.

Analysis of *SHOC2* mutations

Genomic DNA was extracted from patients' peripheral leukocytes. Exons and flanking intron sequences of *SHOC2* were amplified by PCR with primers based on GenBank sequences (Supplementary Table 1, GenBank accession no. NC_000010.10). The M13 reverse or forward sequence was added to the 5′ end of the PCR primers for use as a sequencing primer. PCR was performed in 15 μl of solution containing 67 mM Tris-HCl (pH 8.8), 6.7 mM $MgCl_2$, 17 mM NH_4SO_4, 6.7 μM EDTA, 10 mM β-mercaptoethanol, 1.5 mM dNTPs, 10% (v/v) dimethylsulfoxide (except fragment 7), 1 μM of each primer, 50 ng genomic DNA and 1 unit of Taq DNA polymerase. The reaction consisted of 37 cycles of denaturation at 94 °C for 20 s, annealing at the indicated temperature for 30 s and extension at 72 °C for 30 s. The PCR products of fragment 1a were gel purified; PCR products of the other fragments were purified using MultiScreen PCR plates (Millipore, Billerica, MA, USA). The purified PCR products were sequenced on an ABI PRISM 3130 automated DNA sequencer (Applied Biosystems, Foster City, CA, USA).

Development of a mutation detection system using the light cycler

Real-time PCR and melting curve analysis to detect the c.4A>G mutation was developed using the LightCycler system (Roche Diagnostics, Mannheim,

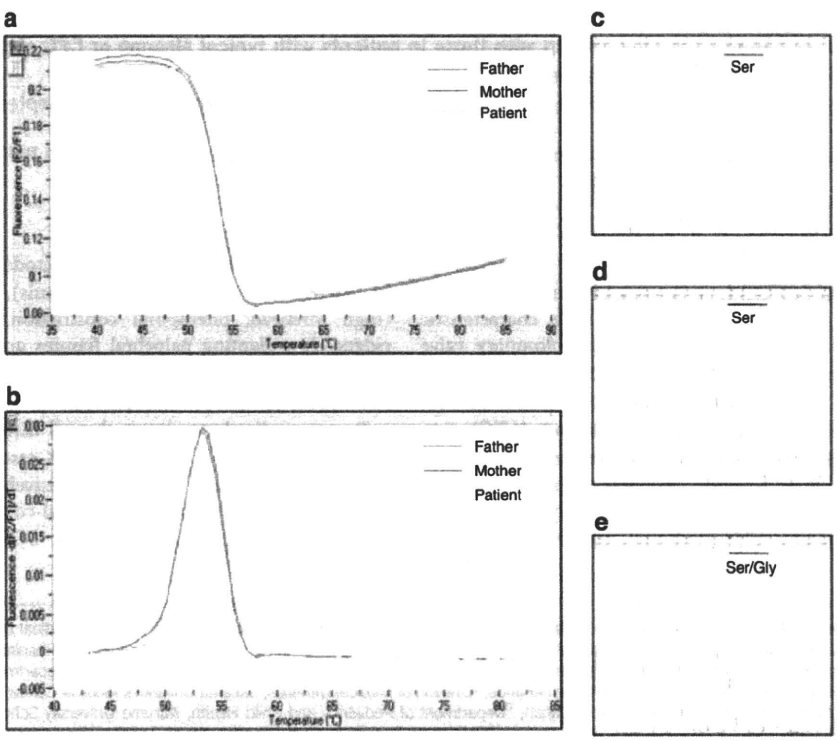

Figure 1 (**a**) PCR followed by melting analysis to detect the c.4A>G mutation. F2 represents the fluorescence emission of the LC Red 640 fluorophore, whereas F1 shows the fluorescence emission of the fluorescein fluorophore. (**b**) Melting curves are automatically converted into melting peaks, which are given as the first negative derivative of the fluorescence (F) versus temperature (T) (-dF/dT) (*y* axis) versus temperature (temp)(*x* axis). The homozygous wild-type allele (parents of NS128) shows a single melting temperature, whereas the heterozygote (NS128) shows two different melting temperatures. (**c**, **d**) Sequencing traces of parents of NS128. (**e**) Sequencing trace of NS128.

Germany). Primer and probe sequences are shown in Supplementary Table 2. The acceptor probe, which matches the mutant allele sequence, was labeled at its 3′ end with fluorescein isothiocyanate. The donor probe was labeled at its 5′ end with LC Red640 and phosphorylated at its 3′ end to prevent probe elongation by the Taq polymerase. Probes were designed by Nihon Gene Research Laboratories (Sendai, Japan). Amplification was performed in a final volume of 20 μl in glass capillaries containing 10 ng of sample DNA, 2 μl of 10× LightCycler-FastStart DNA Master HybProbe (Roche Diagnostics), 12 nM $MgCl_2$, 0.3 μM of each forward and reverse primer and 0.2 μM of each acceptor and donor hybridization probe. PCR was performed under the following conditions: initial denaturation at 95 °C for 10 min, 40 cycles of 95 °C for 10 s, 60 °C for 15 s and 72 °C for 7 s with a ramping time of 20 °C s^{-1}. After amplification, melting curve analysis was performed under the following conditions: 95 °C with 0-s hold, cooling to 40 °C for 30 s and slowly heating the sample to 85 °C with a ramp rate of 0.4 °C s^{-1}.

Real-time quantitative PCR

MTC Multiple Tissue cDNA panels Human 1, 2, Human Fetal, Human Immune and Human Cell Line (Clontech, Palo Alto, CA, USA) were used to evaluate the relative expression of *SHOC2* in various tissues. Separation of mononuclear and polymorphonuclear (PMN) leukocytes from whole blood was performed using Polymorphoprep (Nycomed, Oslo, Norway); total RNA was prepared with the RNeasy Mini Kit (Qiagen, Hilden, Germany). One hundred ng of total RNA was used to synthesize complementary DNA (cDNA) using the High Capacity cDNA Reverse Transcription kit (ABI). Primers for real-time PCR were designed using software provided by Roche (https://www.roche-applied-science.com) (Supplementary Table 3). Universal ProbeLibrary #42 and #60 (Roche) were used for *SHOC2* and *GAPDH*, respectively. PCR was performed in 20 μl of solution containing 10 μl FastStart Universal Probe Master (Rox) (Roche), 18 pmol of each primer, 5 μl cDNA and 0.25 μM universal HybProbe. The reaction conditions were 50 °C for 2 min and 95 °C for 10 min, followed by 40 cycles of 95 °C for 15 s and 60 °C for 11 min. The real-time PCR program was run by the 7500 Real-Time PCR system (ABI). Diluted control cDNA (1:1, 1:10, 1:100, 1:1000 and 1:10 000) from Multiple Tissue cDNA panels (Clontech) was amplified with each reaction in order to generate a standard curve and calculate relative gene expression of *SHOC2*.

RESULTS

Mutation analysis in patients and development of a rapid mutation detection system

Sequence analysis of all coding regions of *SHOC2* in 92 patients revealed a c.4A>G mutation (p.S2G) in exon1 of *SHOC2* in eight unrelated patients. Parental samples were available in three families; the mutation was not identified in parents, suggesting that the mutation occurred *de novo*.

Our results and the previous report identified a c.4A>G mutation in patients with Noonan-like syndrome. To further characterize the occurrence of this mutation, we developed a rapid mutation detection system using a Lightcycler. Two probes were generated for melting curve analysis, and melting curve analysis was performed after PCR. The PCR products from a patient heterozygous for the c.4A>G mutation differed from those obtained from the patient's parents as well as from those obtained from control subjects (Figures 1a and b). The PCR products were verified by sequencing (Figures 1c–e).

Clinical manifestations of patients with the *SHOC2* mutation

The clinical manifestations of eight patients with the *SHOC2* mutation are shown in Table 1; photographs of five of these patients are shown in Figure 2. The ages of the patients ranged from 4 to 25 years. The primary diagnoses for these patients were Costello, Noonan or CFC syndrome. Three had perinatal abnormalities, including tachypnea, hydramnios, pulmonary hemorrhage and intracranial hemorrhage.

Table 1 Clinical manifestations in *SHOC2* mutation-positive patients

Patient ID	*NS34*	*NS93*	*NS97*	*NS121*	*NS128*	*NS180*	*NS220*	*NS232*
SHOC2 mutation	p.S2G	p.S2G	p.S2G	p.S2G	p.S2G	p.S2G	p.S2G	p.S2G
Genotype of father/mother	WT/WT	ND	ND	ND	WT/WT	ND	ND	WT/WT
Gender	M	F	F	M	F	M	F	M
Age (years)	13.8	21	10	5.7	8	9	4	25
Country	Japan	The Netherlands	Japan	Japan	Japan	Japan	Japan	Japan
Primary diagnosis	NS/CFC	CFC	CFC	CFC	CFC	NS	CS	CS
Perinatal abnormality	+	ND	–	–	–	+	+	–
Polyhydramnios	–	ND	–	–	–	+	–	–
Birth weight	3118 g	3360 g	3068 g	2865 g	2308 g	3258 g	3160 g	3090 g
Others	Tachypnea					Pulmonary hemorrhage	Intracranial hemorrhage	
Growth and development								
Failure to thrive	+	+	+	+	+	+	+	+
Mental retardation	+ WISC III at 9 years 3 months VIQ 81, PIQ 87, FIQ 82	–	+ (DQ44)	+ (DQ48)	+ (DQ 66)	+ WISC III at 9 years 4 months VIQ 61, PIQ <40 FIQ 45	+ (DQ53)	+ (IQ65)
Hyperactivity	–	–	+	–	–	–	–	– (irritability in infancy)
Delayed independent walking (age)	+ (3.6 years)	–	+ (1.8 years)	+ (2.8 years)	+ (4 years)	+ (5 years)	+ (4 years)	+ (3.6 years)
Craniofacial characteristics								
Relative macrocephaly	+	+	+	+	+	+	+	+
Hypertelorism	+	–	–	–	–	+	–	+

Table 1 Continued

Patient ID	*NS34*	*NS93*	*NS97*	*NS121*	*NS128*	*NS180*	*NS220*	*NS232*
Downslanting palpebral fissures	+	+	+	–	–	+	–	–
Ptosis	–	+	–	+	–	–	–	–
Epicanthal folds	–	–	+	+	–	+	+	±
Low-set ears	+	+	+	+	+	+	+	+
Highly arched palate	+	+	–	+	+	–	+	+
Prominent forehead	ND	–	+	+	ND	ND	+	ND
Broad forehead	+	+	+	+	+	+	+	ND
Skeletal characteristics								
Short stature	–3.4 s.d. at 13 years	–3 s.d. at 21 years	–4 s.d. at 6 years	–3 s.d. at 1 year 9 months	–5 s.d. at 8 years	–6 s.d. at 9 years	–4.5 s.d. at 3 years 3 months	–2 s.d. at 23 years
Short neck	+	+	–	+	+	+	–	+
Webbing of neck	+	+	–	–	–	–	–	±
Cubitus valgus	+	+	–	–	–	–	–	–
Pectus anomalies	ND	–	+	+	–	+	–	–
Cardiac defects								
Hypertrophic cardiomyopathy	–	–	+	–	+	+	±	–
Atrial septal defect	–	–	+	–	–	–	+	+
Ventricular septal defect	–	–	–	–	–	–	–	+
Pulmonary stenosis	+	–	+	–	+	–	+	–
Mitral valve anomaly	+	–	–	–	–	–	–	+
Others	Pulmonary regurgitation	Arrhythmia						Hypoplasia of papillary muscle
Hair anomalies								
Curly hair	–	–	+	+	+	+	+	+
Sparse hair	+	+	+	+	+	+	+	+
Easily pluckable hair	+	+	+	+	+	ND	+	+
Skin anomalies								
Dark skin	+	+	+	+	+	+	+	+
Hyperkeratosis	ND	+	+	+	+	–	–	+
Hyperelastic skin	+	–	+	+	+	–	–	+
Café-au-lait spots	+	–	–	–	–	–	–	–
Lentigines	+	–	–	–	–	+	–	–
Atopic skin/eczema	+	+	+	+	+	+	+	+
Others					Deep palmar/ planter creases			Facial erythema, nummular eczema
Genital abnormalities	+ (Cryptorchidism)	–	–	–	–	+(Cryptorchidism)	–	–
Blood test abnormality								
Coagulation defect (normal range)	+[a]	ND	–	+[b]	ND	+[c]	–	–
Number of white blood cells(/μl)	7200	8400	16 000	5300	10 900	9900	10 300	9900
(normal range for patient's age)	(5000–10 000)	(5000–10 000)	(4500–13 500)	(6000–15 000)	(4500–13 500)	(4500–13 500)	(6000–15 000)	(5000–10 000)
Polymorph nuclear cell (%)	60 (55)	ND	79 (55)	ND	50 (55)	72 (55)	53 (45)	77 (55)
(mean for each patient's age)								
IgE (U ml $^{-1}$)	ND	ND	2300	94	ND	1800	ND	820
Hypernasal/hoarse voice	ND	–	+	+	–	ND	+	+
Miscellaneous	GH deficiency	Delayed puberty, EEG abnormalities, easy bruising	GH deficiency	GH deficiency	Adenoid hypertrophy, GH deficiency		Dilatation of cerebral ventricles, epilepsy	Congenital hydro-nephrosis, frostbite in winter

Abbreviations: APTT, activated partial thrombin time; AT, antithorombin; BT, bleeding time; CFC, cardio-facio-cutaneous; CS, Costello syndrome; DQ, developmental quotient; EEG, electroencephalogram; FIQ, Full Scale intelligence quotient; GH, growth hormone; ND, not described; NS, Noonan syndrome; PIQ, Performance intelligence quotient; PT, prothrombin time; VIQ, verbal intelligence quotient; WISC, Wechsler Intelligence Scale for Children; WT, wild type.
[a]The test was performed when bloody stool was observed at 7 years of age. BT 180 sec (2.5–13), PT 11.5 sec (10.1–12.0) APTT 62.5 sec (26–37), Factor VIII 53% (52–120). Parenthesis represents normal range for the patient's age.
[b]APTT 54 sec (26–37), Factor IX 22% (47–104), Factor XII 34% (64–129), Factor XIII 51 (72–143). Parenthesis represents normal range for the patient's age.
[c]APTT 57 sec (26–37). Parenthesis represents normal range for the patient's age.

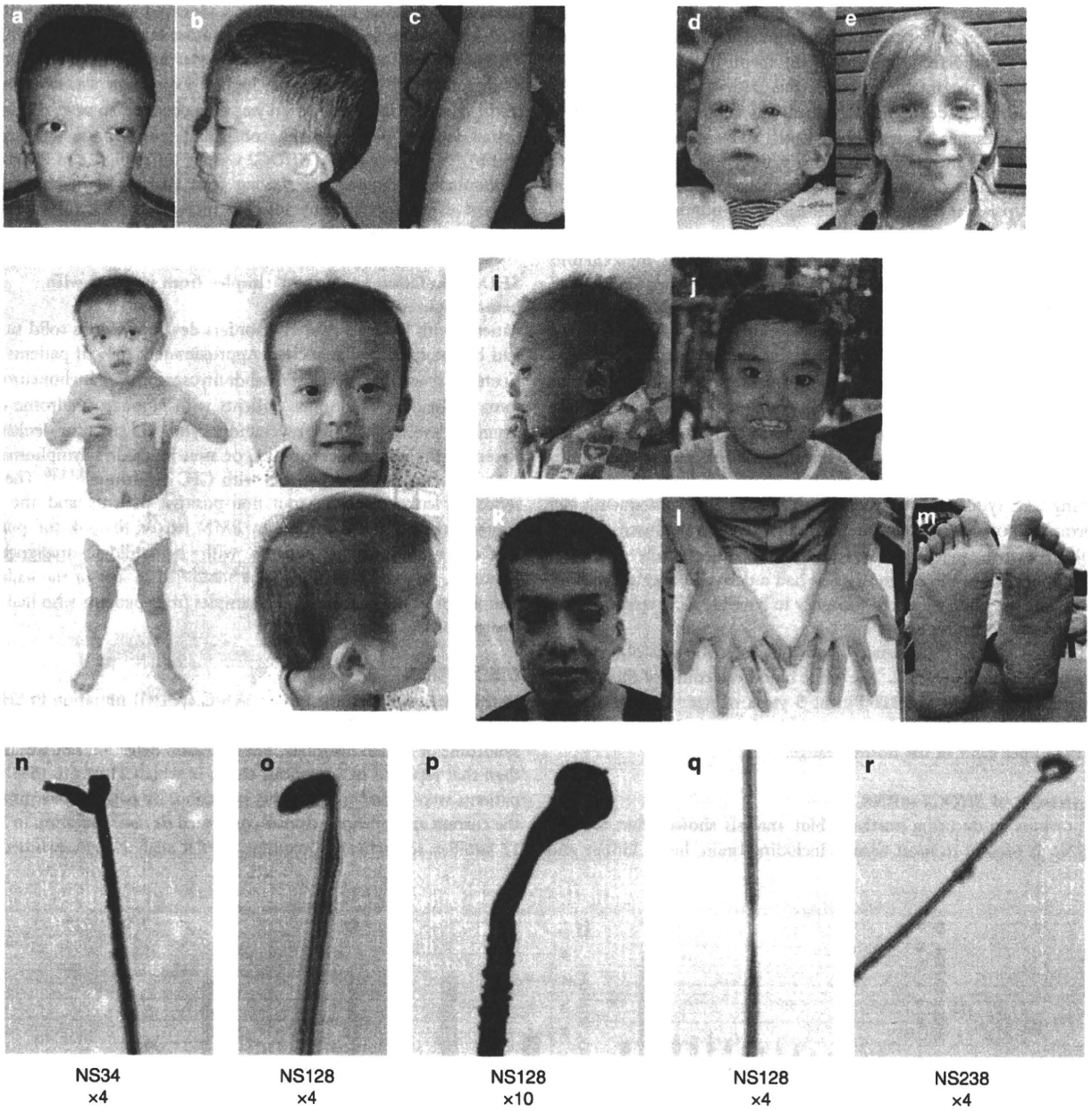

Figure 2 (**a**, **b**) Facial appearance of NS34 at the age of 13 years. (**c**) Dry and atopic skin seen in NS34. (**d**, **e**) NS93. (**f–h**) NS97. (**i**, **j**) NS128. (**k–m**) NS232 at the age of 25 years. (**l**, **m**) Palms and soles of NS232 showing fine wrinkling. Light micrographs of hairs from patients NS34 (**n**), NS128 (**o–q**) and NS238 (**r**). The hair bulb is distorted at an acute angle to the hair shaft, a characteristic described as 'mousetail deformity.' The hair shaft is twisted and longitudinally grooved.

All showed short stature $\geqslant -2$ s.d.) despite normal growth during the fetal period. Mild-to-moderate mental retardation was observed in seven patients. It is of note that delayed independent walking was observed in seven patients. The facial appearances of these patients changed with age. Features frequently observed were relative macrocephaly (8/8 patients), low-set ears (8/8), highly arched palate (6/8) and broad forehead (7/7). Cardiac abnormalities included hypertrophic cardiomyopathy in four patients, atrial septal defect in three patients, pulmonic stenosis in four patients and mitral valve anomaly in two patients. Atopic skin and eczema were observed in all eight patients (Figure 2c), and serum immunoglobulin E level was elevated in three patients. Seven patients had sparse and easily pluckable hair. The hair bulb was bent at an acute angle to the hair shaft, which was irregular and twisted (Figures 2n–r). Four patients had hyponasal/hoarse voice as previously described[18] and three patients showed coagulation defects with prolonged activated partial thrombin time.

The clinical history of two adult patients, NS232 and NS93, differed from those of patients typical for Noonan syndrome. NS232 was a 25-year-old patient, the first son of unrelated healthy parents. Delivery

at 40 weeks was uncomplicated, and birth weight was 3090 g. At 1 month of age, this patient was diagnosed as having an atrioventricular septal defect; the defect spontaneously closed at 5 months of age. During the infantile period, this patient showed irritability and mental/motor delay: head control was achieved at 1 year and 10 months, sitting at 2 years and 4 months and walking at 3 years and 6 months. At his infantile period, this patient was suspected to have Noonan syndrome or Costello syndrome. Pyelostomy for congenital hydronephrosis was performed at the age of 10 months. At 23 years of age, mitral valve replacement was performed because of mitral valve prolapse (III–IV). The dissected mitral valve showed myxomatous change. At 25 years, this patient shows mild mental retardation and displays a gentle personality. Other characteristics include hypertelorism, a highly arched palate and posteriorly rotated ears. During infancy, his hair was pluckable, but the hair abnormality is now subtle. He possesses variable skin abnormalities including fine wrinkles on the palm and soles as well as erythematous rash on the face and eczematous skin changes on the trunks and extremities together with xerotic skin, which are reminiscent of atopic dermatitis (Figures 2k–m). Another adult patient, NS93, has been diagnosed as having CFC syndrome at 1 year of age (Figure 2d). Subsequently her normal motor development and her cognitive development that fell within normal ranges (but was lower than other family members) shed doubt about this diagnosis. She had a delayed pubertal development. She has quite a marked tendency to have bleeding episodes after surgery and to bruise easily.

Leukocytosis in the absence of obvious infection was observed in one of the patients (NS97). The white blood cell count of this patient ranged from 16 000 to 23 000/μl at 5 years of age. The number of leukocytes of the other patients was within the normal range, but close to the upper limit of the normal range.

Expression of *SHOC2* mRNA

A previous study using northern blot analysis showed that *SHOC2* mRNA is present in most tissues, including brain, heart, kidney and pancreas.[16] Because leukocytosis was observed in a patient with the p.S2G mutation, we examined the relative expression of *SHOC2* in various tissues including blood leukocytes and lymphocytes. In the adult human cDNA panel, the highest expression was observed in testis; relatively high expression was also observed in several immune tissues (spleen, bone marrow, tonsil and lymph node) (Figures 3a and b). The expression of *SHOC2* was six times higher in PMN than mononuclear (Figure 3c). Among fetal tissues, brain showed the highest expression (Figure 3d). No increase in *SHOC2* expression was observed in cultured tumor cells (Figure 3e).

SHOC2 mutation analysis in samples from patients with hematologic malignancies

Patients with Noonan-related disorders develop various solid tumors and hematologic malignancies.[5] Approximately 10% of patients with Costello syndrome develop rhabdomyosarcoma, ganglioneuroblastoma or bladder carcinoma. Patients with Noonan syndrome occasionally develop juvenile myelomonocytic leukemia or leukemia.[2] Recently, the occurrence of ALL or non-Hodgkin's lymphoma has been reported in three patients with CFC syndrome.[5,19,20] The presence of leukocytosis in mutation-positive patients and the high expression of *SHOC2* mRNA in PMN led us to look for possible *SHOC2* mutations in patients with hematologic malignancies. However, no such mutations were identified in any of the leukemia samples or in the genomic DNA samples from patients who had been treated for leukemia.

DISCUSSION

In this study, we identified the c.4A>G (p.S2G) mutation in *SHOC2* in 8 of 92 (9%) otherwise mutation-negative patients with Noonan syndrome or related disorders. The mutation detection rate was higher than that reported in a previous study, in which 21 of 410 (5%) such patients were found to carry this mutation. By parental examination, the current and previous studies confirmed *de novo* mutation in 3 and 12 families, respectively. Quantitative PCR analysis demonstrated that

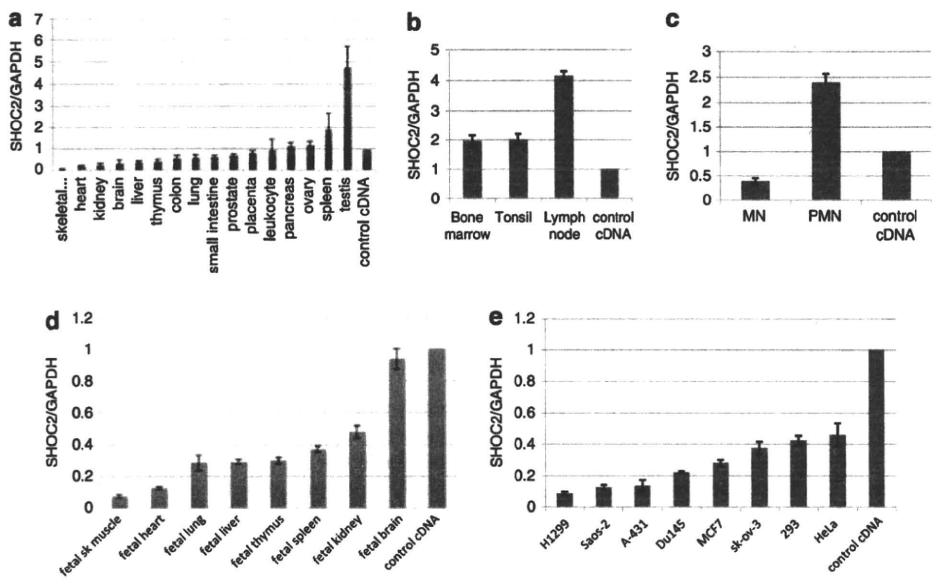

Figure 3 Relative expression of *SHOC2*. Expression levels of *SHOC2* mRNA in various adult human tissues (**a**), adult immune tissues (**b**), human leukocytes (**c**), human fetal tissues (**d**) and human tumor cell lines (**e**) were evaluated by quantitative PCR using *GAPDH* mRNA as the control. Results are expressed as the means and s.d.s of mean values from triplicate samples. Control DNA supplied with Clontech cDNA panels was used as a control.

Table 2 Summary of clinical manifestations in patients with CFC syndrome, Noonan-like syndrome and Noonan syndrome

	CFC syndrome (%)	*Noonan-like syndrome (%)*	*Noonan syndrome (%)*
References	20,21[a]	Cordeddu *et al.*[18] and this study	22
Gene mutations	*KRAS*, *BRAF* and *MAP2K1/2*	*SHOC2*	*PTPN11*, *KRAS*, *SOS1* and *RAF1*
Total patients	63	33	315
Perinatal abnormality			
Polyhydramnios	23/30 (77)	1/7 (14)	21/50 (42)
Fetal macrosomia	ND	ND	20/46 (43)
Growth and development			
Failure to thrive	24/36 (67)	8/8 (100)	51/74 (69)
Mental retardation	25/25 (100)	27/32 (84)	124/293 (42)
Craniofacial characteristics			
Relative macrocephaly	40/58 (69)	31/33 (94)	50/70 (71)
Hypertelorism	17/25 (68)	26/33 (79)	66/82 (80)
Downslanting palpebral fissures fissures fissures	20/25 (80)	4/8 (50)	77/99 (78)
Ptosis	12/25 (48)	24/33 (73)	75/105 (71)
Epicanthal folds	13/25 (52)	5/8 (63)	41/72 (57)
Low-set ears	20/25 (80)	30/33 (91)	115/132 (87)
Skeletal characteristics			
Short stature	46/63 (73)[b]	32/32 (100)	172/297 (58)
Short neck	22/25 (88)	23/33(70)	76/107 (71)
Webbing of neck	6/25(24)	20/33 (61)	84/188 (45)
Cardiac defects			
Hypertrophic cardiomyopathy	24/58 (41)	9/33 (27)	57/277 (21)
Atrial septal defect	11/57 (19)	11/33 (33)	20/69 (29)
Ventricular septal defect	7/57 (12)	3/33(9)	7/70 (10)
Septal defect total	18/57 (32)	14/33 (42)	85/313 (27)
Pulmonic stenosis	23/58 (40)	13/33 (39)	196/312 (63)
Patent ductus arteriosus	ND	0/33 (0)	3/38 (8)
Mitral valve anomaly	10/63 (16)[a]	10/32 (31)	16/67 (24)
Arrhythmia	4/63 (6)	1/33 (3)	14/25 (56)
Skeletal/extremity deformity			
Cubitus valgus	6/25 (24)[a]	2/8 (25)	26/100 (26)
Pectus deformity	27/54 (50)	23/32 (72)	184/287 (64)
Skin/hair anomaly			
Curly hair	58/63 (92)	6/8 (75)	30/75 (40)
Sparse hair	56/63 (89)	33/33 (100)	ND
Loose anagen hair/easily pluckable hair	ND	19/19(100)	ND
Hyperelastic skin	7/25 (28)[a]	5/8 (63)	16/51 (31)
Café-au-lait spots	13/58 (22)[a]	1/8 (13)	5/49 (10)
Lentigines	ND	2/8 (25)	3/49 (6)
Nevus	37/62 (60)[a]	ND	12/46 (26)
Genitalia			
Cryptorchidism	11/41(27)[a]	8/25 (32)	114/211 (54)
Blood test abnormality			
Coagulation defects	1[c]	9/29 (31)	65/180 (36)

Abbreviations: CFC, cardio-facio-cutaneous; ND, not described.
[a]Includes our unpublished data.
[b]Includes short stature (height below the 3rd centile).
[c]A patient with von Willebrand disease was reported.

SHOC2 mRNA is abundant in adult testis and immune tissues as well as in fetal brain. The c.4A>G (p.S2G) mutation was not detected in 82 samples from patients with leukemia.

Clinical manifestations in *SHOC2* mutation-positive patients often vary, even among patients who have a common p.S2G mutation (Table 2 and Supplementary Table 4). In this study and in a previous study, relative macrocephaly (94%), hypertelorism (79%), low-set ears (91%) and short stature (100%) were frequently observed in patients with the *SHOC2* p.S2G mutation.[18] Growth hormone deficiency was observed in 70% of patients. With respect to cardiac abnormalities, pulmonic stenosis was observed in 13 of 33 patients (39%), followed by atrial septal defect (33%), mitral valve anomaly (31%) and hypertrophic cardiomyopathy (27%). Dark skin and atopic dermatitis were seen in 75 and 48% of patients, respectively. Hair abnormalities, including sparse hair (100%) and loose anagen hair/easily pluckable hair (100%), were the most characteristic clinical features of *SHOC2* mutation-positive patients.

The symptomatology of patients with the *SHOC2* mutation does not fit existing disorders, including Noonan, Costello and CFC syndrome. In this paper, we summarize the clinical manifestations of patients with CFC syndrome[21,22] or Noonan syndrome,[23] as described in previous reports, as well as *SHOC2* mutation-positive patients (Table 2). The high frequencies of mental retardation (84%) and sparse hair (100%) observed in *SHOC2* mutation-positive patients are similar to those observed in CFC patients (100 and 89%, respectively); the frequency of mental retardation was higher than that in patients with Noonan syndrome (42%). With respect to cardiac abnormalities, the frequencies of hypertrophic cardiomyopathy, atrial septal defect and mitral valve anomaly are similar to those among patients with Noonan syndrome. However, pulmonic stenosis (39%) was less frequent in *SHOC2* mutation-positive patients than in patients with Noonan syndrome (63%). It is of note that short stature (100%) and pectus deformity (72%) were found to be most frequent in patients with the *SHOC2* mutation. Furthermore, loose anagen/easily pluckable hair has not been reported in mutation-positive patients with Noonan, CFC or Costello syndrome. Taken together, these results suggest that clinical manifestations in patients with *SHOC2* partially overlap with those of Noonan syndrome and CFC syndrome. The presence of easily pluckable/loose anagen hair is distinctive in *SHOC2* mutation-positive patients.

Loose anagen hair has been observed in an isolated loose anagen hair syndrome (OMIM 600628)[24] and has been found to be associated with Noonan syndrome.[25,26] The pathogenesis of loose anagen hair remains unknown. A scalp biopsy in a patient with loose anagen hair showed marked cleft formation between the inner root and the irregularly shaped hair shafts. Abnormalities in the keratin gene have been suggested.[24] Functional analysis of the *SHOC2* p.S2G mutant showed that the mutant protein was aberrantly localized in the membrane fraction after stimulation with epidermal growth factor and induced extracellular signal-regulated kinase signaling in a cell-specific manner.[18] It is possible that dysregulated proliferation or cell-to-cell attachment causes the detachment between inner sheaths and hair shafts.

One of our mutation-positive patients exhibited a remarkable leukocytosis ranging from 12 000 to 24 600/mm^3. Other patients also showed mild leukocytosis, which is near the upper range of the normal levels for their age. This observation led us to examine the tissue and cellular expression of *SHOC2*. In adult tissues, the highest *SHOC2* expression was observed in testis; relatively high expression was also observed in several immune tissues, including spleen, bone marrow, tonsil and lymph node. Among leukocytes, the expression of *SHOC2* was six times higher in PMN than in mononuclear, suggesting that *SHOC2* might be important to the proliferation or survival of PMN leukocytes. We did not identify the p.S2G mutation in 82 samples from patients with hematologic malignancies. A recent study reported that no *SHOC2* mutations were identified in 22 patients with juvenile myelomonocytic leukemia.[27] It is possible that the absence of mutation was due to the relatively small sample size. Alternatively, the gain of function of *SHOC2* might not have leukemogenic potential, and other factors such as aberrant cytokine production may be associated with leukocytosis.

In summary, we identified the *SHOC2* p.S2G mutation in eight patients with Noonan-like syndrome. Analysis of the detailed clinical manifestations of these patients showed that relative macrocephaly, hypertelorism, low-set ears, short stature, sparse/easily pluckable hair and a variety of skin abnormalities, including dark skin and atopic dermatitis, are frequently observed in patients positive for this mutation. A previous study and this study show that only one mutation (p.S2G) is causative for the phenotype. The rapid detection system for the *SHOC2* p.S2G mutation using the Lightcycler will be a useful tool to screen for this mutation in patient samples.

ACKNOWLEDGEMENTS

We thank the patients and families who participated in this study as well as the doctors who referred the patients. This work was supported by Grants-in-Aids from the Ministry of Education, Culture, Sports, Science and Technology of Japan, Japan Society for the Promotion of Science and The Ministry of Health Labour and Welfare to YM and YA.

1 Allanson, J. E., Hall, J. G., Hughes, H. E., Preus, M. & Witt, R. D. Noonan syndrome: the changing phenotype. *Am. J. Med. Genet.* **21,** 507–514 (1985).
2 van der Burgt, I. Noonan syndrome. *Orphanet. J. Rare Dis.* **2,** 4 (2007).
3 Hennekam, R. C. Costello syndrome: an overview. *Am. J. Med. Genet. C Semin. Med. Genet.* **117,** 42–48 (2003).
4 Reynolds, J. F., Neri, G., Herrmann, J. P., Blumberg, B., Coldwell, J. G., Miles, P. V. *et al.* New multiple congenital anomalies/mental retardation syndrome with cardio-facio-cutaneous involvement–the CFC syndrome. *Am. J. Med. Genet.* **25,** 413–427 (1986).
5 Aoki, Y., Niihori, T., Narumi, Y., Kure, S. & Matsubara, Y. The RAS/MAPK syndromes: novel roles of the RAS pathway in human genetic disorders. *Hum. Mutat.* **29,** 992–1006 (2008).
6 Bentires-Alj, M., Kontaridis, M. I. & Neel, B. G. Stops along the RAS pathway in human genetic disease. *Nat. Med.* **12,** 283–285 (2006).
7 Pandit, B., Sarkozy, A., Pennacchio, L. A., Carta, C., Oishi, K., Martinelli, S. *et al.* Gain-of-function RAF1 mutations cause Noonan and LEOPARD syndromes with hypertrophic cardiomyopathy. *Nat. Genet.* **39,** 1007–1012 (2007).
8 Razzaque, M. A., Nishizawa, T., Komoike, Y., Yagi, H., Furutani, M., Amo, R. *et al.* Germline gain-of-function mutations in RAF1 cause Noonan syndrome. *Nat. Genet.* **39,** 1013–1017 (2007).
9 Roberts, A. E., Araki, T., Swanson, K. D., Montgomery, K. T., Schiripo, T. A., Joshi, V. A. *et al.* Germline gain-of-function mutations in SOS1 cause Noonan syndrome. *Nat. Genet.* **39,** 70–74 (2007).
10 Schubbert, S., Zenker, M., Rowe, S. L., Boll, S., Klein, C., Bollag, G. *et al.* Germline KRAS mutations cause Noonan syndrome. *Nat. Genet.* **38,** 331–336 (2006).
11 Tartaglia, M., Mehler, E. L., Goldberg, R., Zampino, G., Brunner, H. G., Kremer, H. *et al.* Mutations in PTPN11, encoding the protein tyrosine phosphatase SHP-2, cause Noonan syndrome. *Nat. Genet.* **29,** 465–468 (2001).
12 Tartaglia, M., Pennacchio, L. A., Zhao, C., Yadav, K. K., Fodale, V., Sarkozy, A. *et al.* Gain-of-function SOS1 mutations cause a distinctive form of Noonan syndrome. *Nat. Genet.* **39,** 75–79 (2007).
13 Aoki, Y., Niihori, T., Kawame, H., Kurosawa, K., Ohashi, H., Tanaka, Y. *et al.* Germline mutations in HRAS proto-oncogene cause Costello syndrome. *Nat. Genet.* **37,** 1038–1040 (2005).
14 Niihori, T., Aoki, Y., Narumi, Y., Neri, G., Cave, H., Verloes, A. *et al.* Germline KRAS and BRAF mutations in cardio-facio-cutaneous syndrome. *Nat. Genet.* **38,** 294–296 (2006).
15 Rodriguez-Viciana, P., Tetsu, O., Tidyman, W. E., Estep, A. L., Conger, B. A., Cruz, M. S. *et al.* Germline mutations in genes within the MAPK pathway cause cardio-facio-cutaneous syndrome. *Science.* **311,** 1287–1290 (2006).

16 Selfors, L. M., Schutzman, J. L., Borland, C. Z. & Stern, M. J. soc-2 encodes a leucine-rich repeat protein implicated in fibroblast growth factor receptor signaling. *Proc. Natl Acad. Sci. USA* **95,** 6903–6908 (1998).
17 Rodriguez-Viciana, P., Oses-Prieto, J., Burlingame, A., Fried, M. & McCormick, F. A phosphatase holoenzyme comprised of Shoc2/Sur8 and the catalytic subunit of PP1 functions as an M-Ras effector to modulate Raf activity. *Mol. Cell.* **22,** 217–230 (2006).
18 Cordeddu, V., Di Schiavi, E., Pennacchio, L. A., Ma'ayan, A., Sarkozy, A., Fodale, V. *et al.* Mutation of SHOC2 promotes aberrant protein N-myristoylation and causes Noonan-like syndrome with loose anagen hair. *Nat. Genet.* **41,** 1022–1026 (2009).
19 Makita, Y., Narumi, Y., Yoshida, M., Niihori, T., Kure, S., Fujieda, K. *et al.* Leukemia in cardio-facio-cutaneous (CFC) syndrome: a patient with a germline mutation in BRAF proto-oncogene. *J. Pediatr. Hematol. Oncol.* **29,** 287–290 (2007).
20 Ohtake, A., Aoki, Y., Saito, Y., Niihori, T., Shibuya, A., Kure, S. *et al.* Non-Hodgkin lymphoma in a patient with cardio-facio-cutaneous syndrome. *J. Pediatr. Hematol. Oncol.* (e-pub ahead of print 2 June 2010).
21 Armour, C. M. & Allanson, J. E. Further delineation of cardio-facio-cutaneous syndrome: clinical features of 38 individuals with proven mutations. *J. Med. Genet.* **45,** 249–254 (2008).
22 Narumi, Y., Aoki, Y., Niihori, T., Neri, G., Cave, H., Verloes, A. *et al.* Molecular and clinical characterization of cardio-facio-cutaneous (CFC) syndrome: overlapping clinical manifestations with Costello syndrome. *Am. J. Med. Genet. A.* **143A,** 799–807 (2007).
23 Kobayashi, T., Aoki, Y., Niihori, T., Cave, H., Verloes, A., Okamoto, N. *et al.* Molecular and clinical analysis of RAF1 in Noonan syndrome and related disorders: dephosphorylation of serine 259 as the essential mechanism for mutant activation. *Hum. Mutat.* **31,** 284–294 (2010).
24 Tosti, A. & Piraccini, B. M. Loose anagen hair syndrome and loose anagen hair. *Arch. Dermatol.* **138,** 521–522 (2002).
25 Mazzanti, L., Cacciari, E., Cicognani, A., Bergamaschi, R., Scarano, E. & Forabosco, A. Noonan-like syndrome with loose anagen hair: a new syndrome? *Am. J. Med. Genet. A.* **118A,** 279–286 (2003).
26 Tosti, A., Misciali, C., Borrello, P., Fanti, P. A., Bardazzi, F. & Patrizi, A. Loose anagen hair in a child with Noonan's syndrome. *Dermatologica.* **182,** 247–249 (1991).
27 Flotho, C., Batz, C., Hasle, H., Bergstrasser, E., van den Heuvel-Eibrink, M. M., Zecca, M. *et al.* Mutational analysis of SHOC2, a novel gene for Noonan-like syndrome, in JMML. *Blood.* **115,** 913 (2010).

Supplementary Information accompanies the paper on Journal of Human Genetics website (http://www.nature.com/jhg)

RESEARCH ARTICLE

Human Mutation

OFFICIAL JOURNAL
HGVS
HUMAN GENOME VARIATION SOCIETY
www.hgvs.org

Molecular and Clinical Analysis of *RAF1* in Noonan Syndrome and Related Disorders: Dephosphorylation of Serine 259 as the Essential Mechanism for Mutant Activation

Tomoko Kobayashi,[1] Yoko Aoki,[1]* Tetsuya Niihori,[1] Hélène Cavé,[2] Alain Verloes,[2] Nobuhiko Okamoto,[3] Hiroshi Kawame,[4,5] Ikuma Fujiwara,[6] Fumio Takada,[7] Takako Ohata,[7] Satoru Sakazume,[8] Tatsuya Ando,[9] Noriko Nakagawa,[10] Pablo Lapunzina,[11] Antonio G. Meneses,[11] Gabriele Gillessen-Kaesbach,[12] Dagmar Wieczorek,[13] Kenji Kurosawa,[14] Seiji Mizuno,[15] Hirofumi Ohashi,[16] Albert David,[17] Nicole Philip,[18] Afag Guliyeva,[1] Yoko Narumi,[1] Shigeo Kure,[1,6] Shigeru Tsuchiya,[6] and Yoichi Matsubara[1]

[1]Department of Medical Genetics, Tohoku University School of Medicine, Sendai, Japan; [2]APHP, Hôpital Robert Debré, Département de Génétique; Université Paris 7-Denis Diderot, Paris, France; [3]Department of Medical Genetics, Osaka Medical Center and Research Institute for Maternal and Child Health, Izumi, Osaka, Japan; [4]Division of Medical Genetics, Nagano Children's Hospital, Nagano, Japan; [5]Department of Genetic Counseling, Ochanomizu University, Tokyo, Japan; [6]Department of Pediatrics, Tohoku University School of Medicine, Sendai, Japan; [7]Department of Medical Genetics, Kitasato University Graduate School of Medical Sciences, Sagamihara, Japan; [8]Division of Medical Genetics, Gunma Children's Medical Center, Gunma, Japan; [9]Department of Pediatrics, Jikei University School of Medicine, Tokyo, Japan; [10]Department of Pediatrics, National Defense Medical College, Tokorozawa, Saitama, Japan; [11]Servicio de Genetica Medica, Hospital Universitario La Paz, Madrid, Spain; [12]Institut für Humangenetik Lübeck, Universitätsklinikum Schleswig-Holstein, Lübeck, Germany; [13]Institut für Humangenetik, Universitaetsklinikum Essen Universitaet Duisburg-Essen, Essen, Germany; [14]Division of Medical Genetics, Kanagawa Children's Medical Center, Yokohama, Japan; [15]Department of Pediatrics, Central Hospital, Aichi Human Service Center, Aichi, Japan; [16]Division of Medical Genetics, Saitama Children's Medical Center, Saitama, Japan; [17]CHU Nantes, Nantes, France; [18]Hôpital de la Timone, Marseille, France

Communicated by Nancy B. Spinner

Received 20 July 2009; accepted revised manuscript 2 December 2009.
Published online in Wiley InterScience (www.interscience.wiley.com). DOI 10.1002/humu.21187

ABSTRACT: Noonan syndrome (NS) and related disorders are autosomal dominant disorders characterized by heart defects, facial dysmorphism, ectodermal abnormalities, and mental retardation. The dysregulation of the RAS/MAPK pathway appears to be a common molecular pathogenesis of these disorders: mutations in *PTPN11*, *KRAS*, and *SOS1* have been identified in patients with NS, those in *KRAS*, *BRAF*, *MAP2K1*, and *MAP2K2* in patients with CFC syndrome, and those in *HRAS* mutations in Costello syndrome patients. Recently, mutations in *RAF1* have been also identified in patients with NS and two patients with LEOPARD (multiple lentigines, electrocardiographic conduction abnormalities, ocular hypertelorism, pulmonary stenosis, abnormal genitalia, retardation of growth, and sensorineural deafness) syndrome. In the current study, we identified eight *RAF1* mutations in 18 of 119 patients with NS and related conditions without mutations in known genes. We summarized clinical manifestations in patients with *RAF1* mutations as well as those in NS patients with *PTPN11*, *SOS1*, or *KRAS* mutations previously reported. Hypertrophic cardiomyopathy and short stature were found to be more frequently observed in patients with *RAF1* mutations. Mutations in *RAF1* were clustered in the conserved region 2 (CR2) domain, which carries an inhibitory phosphorylation site (serine at position 259; S259). Functional studies revealed that the RAF1 mutants located in the CR2 domain resulted in the decreased phosphorylation of S259, and that mutant RAF1 then dissociated from 14-3-3, leading to a partial ERK activation. Our results suggest that the dephosphorylation of S259 is the primary pathogenic mechanism in the activation of RAF1 mutants located in the CR2 domain as well as of downstream ERK.
Hum Mutat 30:1–11, 2010. © 2010 Wiley-Liss, Inc.

KEY WORDS: RAS; MAPK; RAF1; Noonan syndrome; PTPN11; hypertrophic cardiomyopathy

Introduction

Noonan syndrome (NS; MIM# 163950) is an autosomal dominant developmental disorder characterized by facial dysmorphism, including hypertelorism, low-set ears, ptosis, short stature, skeletal abnormalities, and heart defects [Allanson et al., 1985; Mendez and Opitz, 1985]. Frequently observed features in NS patients are pulmonary stenosis (PS), hypertrophic cardiomyopathy, chest deformities, a webbed/short neck, mental

Additional Supporting Information may be found in the online version of this article.

Present address of Yoko Narumi: Department of Medical Genetics, Shinshu University School of Medicine, Matsumoto, Japan.

*Correspondence to: Yoko Aoki, Department of Medical Genetics, Tohoku University School of Medicine, 1-1 Seiryo-machi, Sendai 980-8574, Japan.
E-mail: aokiy@mail.tains.tohoku.ac.jp

retardation, genitourinary defects including cryptorchidism in males, and bleeding diathesis due to factor XI deficiency. The incidence of this syndrome is estimated to be 1 in 1,000–2,500 live births. LEOPARD (multiple *l*entigines, *e*lectrocardiographic conduction abnormalities, *o*cular hypertelorism, *p*ulmonary stenosis, *a*bnormal genitalia, *r*etardation of growth, and sensorineural *d*eafness) syndrome (MIM# 151100) is known to be a NS-related disorder [Digilio et al., 2002]. The features of NS overlap with those of Costello syndrome and cardio-facio-cutaneous (CFC) syndrome. Patients with Costello syndrome (MIM# 218040) show distinctive facial features, mental retardation, high birth weight, neonatal feeding problems, curly hair, nasal papillomata, deep skin creases at palms and soles, and hypertrophic cardiomyopathy [Hennekam, 2003]. CFC syndrome (MIM# 115150) is characterized by distinctive facial features, mental retardation, heart defects (PS, atrial septal defect [ASD], and hypertrophic cardiomyopathy), and ectodermal abnormalities such as sparse, friable hair, hyperkeratotic skin lesions, and a generalized ichthyosis-like condition [Reynolds et al., 1986].

The molecular pathogenesis of these syndromes has been investigated. Tartaglia et al. [2001] have identified missense mutations in *PTPN11*, a gene encoding protein tyrosine phosphatase (PTP) SHP-2, in 45% of clinically diagnosed NS patients. Specific mutations in *PTPN11* has been identified in patients with LEOPARD syndrome [Digilio et al., 2002]. In 2005, we identified *HRAS* germline mutations in patients with Costello syndrome [Aoki et al., 2005]. Mutations in *KRAS*, *BRAF*, and *MAP2K1/2* have been identified in those with CFC syndrome [Niihori et al., 2006; Rodriguez-Viciana et al., 2006]. Mutations in *KRAS* and *SOS1* have also been identified in patients with NS [Roberts et al., 2007; Schubbert et al., 2006; Tartaglia et al., 2007]. Mutations in *NF1* and *SPRED1* have been identified in patients with neurofibromatosis type I (MIM# 162200) [Brems et al., 2007]. These findings suggest that dysregulation of the RAS/RAF/MEK/ERK pathway causes NS and related disorders, and thus it has been suggested that these syndromes be comprehensively termed the RAS/MAPK syndromes [Aoki et al., 2008] or the neuro-cardio-facial-cutaneous syndrome [Bentires-Alj et al., 2006].

In 2007, gain-of-function mutations in *RAF1* were identified in 3–17% of patients with NS and two patients with LEOPARD syndrome [Pandit et al., 2007; Razzaque et al., 2007]. RAF1 is a member of the RAF serine–threonine kinase family and transmits the upstream RAS signaling to downstream MEK and ERK. RAF1, ARAF, and BRAF share three conserved regions, CR1, CR2, and CR3 [Mercer and Pritchard, 2003]. Mutations in *BRAF* identified in patients with CFC syndrome are clustered in CR1 and CR3 domains [Aoki et al., 2008]. In contrast, reported *RAF1* mutations in NS and LEOPARD syndrome were located in the CR2 domain and some mutations were located in CR3 domain. These mutants had enhanced RAF1 kinase activities and most mutations, but not all, showed enhanced phosphorylation of ERK1/2 [Pandit et al., 2007; Razzaque et al., 2007]. Pandit et al. [2007] suggested that RAF1 mutations might interfere with RAF1 phosphorylation at serine 259 as well as with 14-3-3 interaction, and reported that p.P261S did not bind to 14-3-3. However, the mechanisms of RAF1 activation in mutants remain unexplained.

In the present study, we analyzed the *RAF1* gene in 119 patients with NS and related phenotypes without mutations in *PTPN11*, *HRAS*, *KRAS*, *BRAF*, *MAP2K1/2*, and *SOS1*. Detailed clinical manifestations in our new patients with *RAF1* mutations were evaluated, and those in patients with *RAF1 KRAS*, *PTPN11*, and *SOS1* mutations previously reported by us and others were examined. Furthermore, we explored the molecular mechanisms by which RAF1 mutants are activated.

Materials and Methods

Patients

One hundred nineteen patients with NS or related phenotypes were recruited. The primary diagnoses made by clinical dysmorphologists and general pediatricians were as follows: 44 patients with NS, 46 patients with CFC syndrome, 25 patients with Costello syndrome, and 4 patients with atypical phenotypes. No mutations in *PTPN11*, *HRAS*, *KRAS*, *BRAF*, *MAP2K1*, *MAP2K2*, or *SOS1* were identified in these patients. Control DNA was obtained from 105 healthy Japanese individuals. Control DNA from 105 healthy Caucasian individuals was purchased from Coriell Cell Repositories (Camden, NJ). This study was approved by the Ethics Committee of Tohoku University School of Medicine. We obtained informed consent from all subjects involved in the study and specific consent for photographs from six patients.

Mutation Analysis in *RAF1*

Genomic DNA was isolated from the peripheral blood leukocytes of the patients. Each exon with flanking intronic sequences in *RAF1* was amplified with primers based on GenBank sequences (Supp. Table S1; GenBank accession no. NC_000003.10). The M13 reverse or forward sequence was added to the 5′ end of the polymerase chain reaction (PCR) primers for use as a sequencing primer. PCR was performed in 30 μl of a solution containing 10 mM Tris-HCl (pH 8.3), 50 mM KCl, 1.5 mM $MgCl_2$, 0.2 mM dNTP, 10% (v/v) DMSO, 24 pmol of each primer, 100 ng genomic DNA, and 1.5 units of Taq DNA polymerase. The reaction conditions consisted of 35 cycles of denaturation at 94°C for 15 sec, annealing at 55°C for 15 sec, and extension at 72°C for 40 sec. The products were gel-purified and sequenced on an ABI PRISM 310 or 3130 automated DNA sequencer (Applied Biosystems, Foster City, CA).

Determination of the RAF1 phosphorylation status

The expression construct, including a *RAF1* cDNA (pUSEamp-*RAF1*), was purchased from Millipore (Billerica, MA). A Myc-tag was introduced at the 5′ terminus of the cDNA by PCR and the PCR product was subcloned into pCR4-TOPO (Invitrogen, Carlsbad, CA). The entire cDNA was verified by sequencing. A single-base substitution resulting in p.H103Q, p.R191I, p.S257L, p.S259F, p.P261A, p.N262K, or p.S427G was introduced using a QuickChange Site-Directed Mutagenesis Kit (Stratagene, La Jolla, CA). All mutant constructs were verified by sequencing. The Myc-tagged wild-type *RAF1* cDNA and mutant cDNAs were digested with *Eco*RI and *Eco*RV and subcloned into the *Eco*RI–*Eco*RV site of the pUSEamp-*RAF1*.

COS7 cells were purchased from the American Type Culture Collection (ATCC, Rockville, MD). Cells were maintained in DMEM containing 10% fetal calf serum (FCS), 50 U/ml penicillin, and 50 μg/ml streptomycin. COS7 cells were seeded at 1×10^5 cells per 6-cm dish, and 24 hr later, 2.0 μg of pUSE vectors encoding one of the wild-type (WT) or mutant RAF1 cDNAs were transfected using 8 μl of PLUS Reagent and 12 μl of Lipofectamine Reagent (Invitrogen). After 3 hr, the medium was replaced to complete medium. After 48-hr culture, cells were scraped and collected by centrifugation after two washes with phosphate-buffered saline

(PBS). Lysates were prepared in 100-μl lysis buffer (10 mM Tris-HCl pH 8.0 and 1% SDS) and boiled for 3 min. The DNA was sheared with a syringe. The lysates were centrifuged at 14,000 × *g* for 15 min at 4°C and protein concentration was determined by Bradford assay. Thirty micrograms of protein was subjected to SDS-polyacrylamide gel electrophoresis (5–20% gradient gel) (ATTO, Tokyo, Japan), transferred to nitrocellulose membrane, and probed with anti-Myc antibody and phospho-specific RAF1 antibodies (Cell Signaling, Danvers, MA). All the membranes were visualized using a Western Lightning ECL-Plus Kit (Perkin-Elmer, Norwalk, CT). The following antibodies were used for Western blotting: anti-Myc (9E10, Santa Cruz Biotech, Santa Cruz, CA), antiphospho-c-Raf (S259) (Cell Signaling), antiphospho-c-Raf (S338) (Millipore), antiphospho-c-Raf (S289/296/301) (Cell Signaling), antiphospho-c-Raf (S621) (Millipore), and antineomycin phosphotransferase II (Millipore).

For immunoprecipitation, lysates were prepared in 1 ml of ice-cold RIPA buffer (50 mM Tris-HCl pH 7.5, 150 mM NaCl, 1 mM EDTA, 1:100 protease inhibitor (Sigma, St. Louis, MO), 1:1000 phosphatase inhibitor (Sigma), and 1% Triton X) and incubated on ice for 15 min. Four hundred micrograms of protein was incubated with anti-Myc (9E10) antibody for 1 hr at 4°C. Immune complexes were collected by adding 50 μl of 50% protein G-Sepharose bead slurry (GE Healthcare, Milwaukee, WI) for 1 hr at 4°C, washed three times with RIPA buffer, and then boiled in 2 × SDS buffer. The samples were resolved in 5–20% gradient polyacrylamide gels, transferred to nitrocellulose membranes and probed with antiphospho-c-Raf (S259) and anti-Myc (9E10) antibodies.

Reporter Assay

NIH 3T3 cells (ATCC) were maintained in DMEM containing 10% newborn calf serum, 50 U/ml penicillin, and 50 μg/ml of streptomycin. One day prior to the transfection, the NIH 3T3 cells were plated in 12-well plates with a density of 1×10^5 cells per well. Cells were transiently transfected using Lipofectamine and PLUS Reagents with 700 ng of pFR-luc, 15 ng of pFA2-Elk1, 7 ng of phRLnull-luc, and 35 ng of WT or mutant expression constructs of *RAF1*. Eighteen hours after transfection, the cells were cultured in DMEM without serum for 24 hr. Cells were harvested in passive lysis buffer, and luciferase activity was assayed using a Dual-Luciferase Reporter Assay System (Promega, Madison, WI). Renilla luciferase expressed by phRLnull-luc was used to normalize the transfection efficiency. The experiments were performed in triplicate. Data are shown as mean ± SD. Statistical analysis was performed using Excel.

Binding of RAF1 with 14-3-3

An expression construct containing Myc- and Flag-tagged 14-3-3 ζ (pCMV6-14-3-3 ζ) was purchased from Origene (Rockville, MD). In order to remove the Myc-tag from the construct, the 3′ half of the cDNA and the Myc-tag were removed by digestion with *Eco*RV and the 3′ half of cDNA was filled using PCR. An S621A mutation, which impairs phosphorylation of S621 to bind 14-3-3, was introduced into pUSE RAF1 harboring WT, p.S257L, or p.N262K cDNA by a Quickchange Site-Directed Mutagenesis Kit. HEK293 cells (ATCC) were transfected with 2 μg RAF1 constructs and 2 μg pCMV6-14-3-3 ζ construct using Lipofectamine and PLUS Reagents. After 48 hr, cells were scraped and collected by centrifugation after two washes with PBS. Lysates were prepared as described above. The Myc-tagged RAF1 was immunoprecipitated with anti-Myc antibody (clone4A6, Millipore) for 1 hr at 4°C. Immune complexes were collected by adding 50 μl of 50% protein G-Sepharose bead slurry (GE Healthcare) for 1 hr at 4°C, washed three times with RIPA buffer, and then boiled in 2 × SDS buffer. The samples were resolved in 5–20% gradient polyacrylamide gels, transferred to nitrocellulose membranes, and probed with anti-FLAG M2 (Sigma) and anti-Myc antibodies. For immunoprecipitation of 14-3-3, anti-FLAG M2 antibody was used and immunoblotting was performed using anti-FLAG M2 and anti-c-Raf (Cell Signaling) antibodies.

Results

Mutation Analysis in Patients

We identified eight amino acid changes in 18 patients (Table 1). A C-to-T nucleotide change, resulting in an amino acid change p.S257L, was identified in 11 patients. Novel p.R191I (c.572G>T) and p.N262K (c.786T>A) were identified in one each patient. Previously reported mutations, including p.S259F (c.776C>T), p.P261A (c.781C>G), p.P261L (c.782C>T), p.S427G (c.1279A>G), and p.L613V (c.1837C>G), were identified in a single patient. Nucleotide numbering reflects cDNA numbering with +1 corresponding to the A of the ATG translation initiation codon in Genbank NM_002880.3, according to journal guidelines (www.hgvs.org/mutnomen). The initiation codon is codon 1. The mutation p.S427G, which has been reported in a patient with therapy-related acute myeloid leukemia [Zebisch et al., 2006], was identified in one patient. None of the newly identified mutations were observed in the control DNA of 105 ethnically matched healthy subjects. Parental samples were obtained from six patients (NS86, 92, 209, 210, 222, and 258). The analysis showed that p.S257L, p.P261A, and p.N262K occurred de novo. p.S427G was also identified as well in his 32-year-old mother, who also exhibited a Noonan phenotype with distinctive facial appearance, sparse hair in infancy, and multiple lentigines. The p.H103Q (c.309C>G) was identified in patient NS86, in whom p.S257L was also identified. This amino acid change was identified in one of his parents without any clinical features, suggesting that this amino acid change was polymorphic.

Clinical Manifestations of Patients with *RAF1* Mutations

Initial diagnoses of patients with *RAF1* mutations were as follows: NS in 11 patients, CFC syndrome in 4 patients, and Costello in 3 patients (Supp. Table S2). Four patients who were first diagnosed as having CFC syndrome were reclassified as NS because of facial features and normal mental development after identification of *RAF1* mutations. Three patients were diagnosed as having Costello syndrome. One patient was rediagnosed as having NS (NS135) and the other patient died at 1 month (NS209). Detailed information on clinical manifestations of NS205 was not available.

Detailed clinical manifestations in 18 patients with *RAF1* mutations were evaluated (Table 2 and Fig. 1). Nine of 15 patients had prenatal abnormality, including cystic hygroma, polyhydramnions, and asphyxia. Most patients had characteristic craniofacial abnormalities frequently observed in NS: relative macrocephaly (94%), hypertelorism (93%), downslanting palpebral fissures (63%), epicanthal folds (86%), and low-set ears (93%). Mental retardation was observed in 6 of 11 (55%) patients. Short stature (73%), short neck (93%), and webbing of neck (81%) were also observed. As for cardiac abnormalities, hypertrophic cardiomyopathy was observed in 10 of 16 patients (63%), followed by pulmonic stenosis (47%),

Table 1. *RAF1* Mutations Identified in This Study*

Patient ID	Country of origin	Final diagnosis	Exon	Nucleotide change	Amino acid change	Domain	Genotype of father/mother
NS213	France	atypical NS	5	c. 572G>T	p.R191I[a]	CR1	NA
NS39	Japan	NS	7	c.770C>T	p.S257L	CR2	NA
NS86	France	NS	3, 7	c.309C>G	p.H103Q	CR1,	H103Q/WT
				c.770C>T	p. S257L	CR2	WT/WT
NS92	Germany	NS	7	c.770C>T	p.S257L	CR2	WT/WT
NS135	Japan	NS	7	c.770C>T	p.S257L	CR2	NA
NS146	Spain	NS	7	c.770C>T	p.S257L	CR2	NA
NS199	Japan	NS	7	c.770C>T	p.S257L	CR2	NA
NS200	France	NS	7	c.770C>T	p.S257L	CR2	NA
NS215	Japan	NS	7	c.770C>T	p.S257L	CR2	NA
NS227	Japan	NS	7	c.770C>T	p.S257L	CR2	NA
NS256	Japan	NS	7	c.770C>T	p.S257L	CR2	NA
NS258	Japan	NS	7	c.770C>T	p.S257L	CR2	WT/WT
NS279	Japan	NS	7	c.776C>T	p.S259F	CR2	NA
NS210	France	NS	7	c.781C>G	p.P261A	CR2	WT/WT
NS205	France	CS[b]	7	c.782C>T	p.P261L	CR2	NA
NS209	France	CS[c]	7	c.786T>A	p.N262K[a]	CR2	WT/WT
NS222	Japan	NS	12	c.1279A>G	p.S427G[d]	CR3	WT/p.S427G
NS285	Japan	NS	17	c.1837C>G	p.L613V	CR3	NA

NS, Noonan syndrome; CS, Costello syndrome; WT, wild type; CR, conserved region; NA, not available.
*GenBank RefSeq: NM_002880.3 Nucleotide numbering reflects cDNA numbering with +1 corresponding to the A of the ATG translation initiation codon in the reference sequence, according to journal guidelines (www.hgvs.org/mutnomen). The initiation codon is codon 1.
[a]Novel mutation.
[b]Detailed clinical manifestations were not obtained.
[c]The patient died at 1 month.
[d]The mutation was previously identified in a patient with a therapy-related acute leukemia.

ASD (31%), arrhythmia (38%), and mitral valve anomaly (29%). Other observed clinical features were hyperelastic skin (58%), curly hair (47%), and cryptorchidism in males (50%). Coagulation defects were observed in two patients.

Four patients with *RAF1* mutations died before 5 years of age (Supp. Table S2). Patient NS39 were diagnosed as having cystic hygroma in the prenatal period and had suffered from neonatal hypertrophic cardiomyopathy. At 1 year of age, she contracted acute respiratory distress syndrome after having pneumonia and died of respiratory failure. Patient NS199 had been suspected to have achondroplasia because of short limbs. He was diagnosed as having NS at 3 years of age because of distinct facial features, growth failure, short stature, and hypertrophic cardiomyopathy. He had pneumonia without fever for a week and died suddenly at 5 years of age. Patient NS227 suffered from feeding difficulties, ectopic atrial tachycardia, as well as VSD and pulmonary hypertension. The patient died at 2 months of tachycardia (>200/min) and laryngeal edema.

Clinical manifestations in our patients with *RAF1* mutations were compared with those previously reported (Table 2). The high frequency of hypertrophic cardiomyopathy in our study (63%) was consistent with that observed in patients with *RAF1* mutations previously reported (77%). The frequency of ASD and that of mitral valve anomaly were similar to those of the previous studies. However, the frequency of PS in our study (47%) was higher than that previously reported (11%). Arrhythmia was less frequently observed in our patients with *RAF1* mutations (38 vs. 89%). The frequency of mental retardation (55%) was almost same as that of the previous studies (56%). Hyperelastic skin (58%) and coagulation defects (two cases) were also described in previously reported patients with *RAF1* mutations (24% and one case, respectively).

Phosphorylation State of Mutant RAF1 Proteins

RAF1 is a ubiquitously expressed RAF serine/threonine kinase, which regulates the RAS pathway. It has been shown that phosphorylation of serine, threonine, and tyrosine residues contributes to a conformational change of RAF1 protein and activation in growth factor stimulation [Mercer and Pritchard, 2003]. In the inactive state, phosphorylated S259 and S621 serve as binding sites for 14-3-3, leading to a closed confirmation [Dhillon et al., 2007]. Phosphorylation of S621 seems essential for RAF1 activation. In contrast, phosphorylation of serine 259 has been shown to have an inhibitory role in RAF1 activation. When cells are stimulated with growth factors, dephosphorylation of S259 by protein phosphatase 1 (PP1) and/or protein phosphatase 2A (PP2A) promotes the dissociation of 14-3-3 from RAF1, resulting in an activated conformation of RAF1 protein. For full activation, multiple residues, including S338, are phosphorylated and substrate of RAF1 enters the catalytic cleft in the CR3 kinase domain. Negative feedback from activated ERK results in the phosphorylation of S289, 296, and 301 [Dhillon et al., 2007].

To examine the phosphoryalation status of mutants observed in NS patients, we transfected constructs harboring WT *RAF1* cDNA and five mutants identified in NS patients. Immunoblotting was performed using four phospho-specific antibodies of RAF1 (Fig. 2A). We first analyzed the phosphorylation status of two phosphorylation sites, S259 and S621, using antibodies that recognize each site. Immunoblotting showed that phosphorylation of S259 was scarcely observed in cell lysates expressing p.S257L and p.N262K. In contrast, phosphorylation of S259 of p.H103Q, p.R191I, and p.S427G was similar to that in WT RAF1. To confirm this observation, immunoprecipitation was performed using an anti-Myc antibody, and phosphorylation levels at S259 were examined (Fig. 2B). Immunoprecipitated RAF1 mutants (p.S257L and p.N262K) were not phosphorylated at S259, confirming that these mutants had impaired phosphorylation of S259. The phosphorylation level of S621 in four mutants (p.H103Q, p.R191I, p.S257L, and p.N262K) was similar to that in WT (Fig. 2A), whereas that in cells expressing p.S427G was enhanced. Phosphorylation levels at S338 and S289/296/301 were similar to that in WT except for p.S427G (Fig. 2A).

Phosphorylation levels at S259, S289/296/301, S338, and S621 were shown to be enhanced in cells expressing p.S427G. The expression of p.S427G appeared enhanced and the band was

Table 2. Clinical Manifestations in *RAF1*-Positive Patients in This Study and Past Studies

	Present cohort (%)	NS with *RAF1* mutations (%)	LS with *RAF1* mutations (%)
Number of patients in total	17	35[a]	2
Perinatal abnormality			
Polyhydramnios	6/15 (40)	6/19 (32)	ND
Fetal macrosomia	5/11 (45)	6/20 (30)	ND
Growth and development			
Failure to thrive in infancy	10/12(83)	3	ND
Mental retardation	6/11 (55)	19/34 (56)	1
Outcome			
Died	4/17 (24)	2/11 (18)	ND
Craniofacial characteristics			
Relative macrocephaly	16/17 (94)	16/21 (76)	ND
Hypertelorism	14/15 (93)	20/21 (95)	2
Downslanting palpebral fissures	10/16 (63)	19/21 (90)	2
Ptosis	9/16 (56)	19/21 (90)	1
Epicanthal folds	12/14 (86)	12/21 (57)	1
Low-set ears	14/15 (93)	18/21 (86)	2
Skeletal characteristics			
Short stature	11/15 (73)	30/35 (86)	2
Short neck	14/15 (93)	21/31 (68)	2
Webbing of neck	13/16 (81)	25/30 (83)	2
Cardiac defects			
Hypertrophic cardiomyopathy	10/16 (63)	27/35 (77)	2
Atrial septal defect	5/16 (31)	11/35 (31)	0
Ventricular septal defect	3/17 (18)	3/35 (9)	0
Pulmonic stenosis	7/15 (47)	4/35 (11)	1
Patent ductus arteriosus	2/17 (12)	ND	ND
Mitral valve anomaly	5/17 (29)	8/32 (25)	2
Arrhythmia	6/16 (38)	8/9 (89)	ND
Others	TR 1, PH 1, atrioventricular valve dysplasia 1, valvular AS 1	polyvalvular dysplasia 2 pulmonary valve dysplasia 1, PFO 1, TOF 2, AS 1, right shaft deflection 1	
Skeletal/extremity deformity			
Cubitus valgus	2/9 (22)	7/22 (32)	2
Pectus deformity	5/13 (38)	20/31 (65)	2
Others		prominent finger pads 2	prominent finger pads 1
Skin/hair anomaly			
Curly hair	8/17 (47)	6/24 (25)	2
Hyperelastic skin	7/12 (58)	5/21 (24)	2
Café au lait spots	1/14 (7)	2/20 (10)	2
Lentigines	1/14 (7)	2/21 (10)	2
Naevus	3/15 (20)	9/22 (41)	0
Others	low posterior implantation 4, hyperpigmentation 3, redundant skin 3, sparse hair 2, sparse eyebrows 2, hemangioma 2	dry skin 3, sparse hair 3, sparse eyebrows 2, keratosis pilaris 2	
Genitalia	6/11 (55)	11/16 (69)	
Cryptorchidism	5/10 (50)	8/13 (62)	ND
Blood test abnormality			
Coagulation defects	2/11 (18)	1/4 (25)	ND

NS, Noonan syndrome; LS, LEOPARD syndrome; ND, not described; TR, tricuspid regurgitation; PH, pulmonary hypertension; AS, aortic stenosis; PFO, patent foramen ovale; TOF, tetralogy of Fallot.

[a]Includes affected family members. Clinical manifestations in 3, 21, and 11 NS patients with *RAF1* mutations were summarized from three reports [Ko et al., 2008; Pandit et al., 2007; Razzaque et al., 2007], respectively.

rather broad. However, Western blotting using antineomycin phosphoacetyltransferase antibody that recognizes the amount of plasmids introduced in cells showed that the transfection efficiency in cells expressing p.S427G was similar to that in cells expressing other mutants (Fig. 2A). These findings were consistently observed in three independent experiments. Recent studies have shown that autophosphorylation of S621 is required to prevent proteasome-mediated degradation [Noble et al., 2008]. To explore the possibility that p.S427G mutant is resistant to proteasome-mediated degradation, we examined the amount of WT RAF1 and p.S427G at 24, 48, and 72 hr after transfection in serum-starved or complete medium (Fig. 2C). The results showed that the expression of Myc-tagged RAF1 in cells expressing p.S427G was similar to that in WT RAF1, although multiple bands were observed, suggesting the hyperphosphorylation of the p.S427G mutant.

ELK Transactivation in Mutant RAF1 Proteins

To examine the effect on the downstream pathway of mutant RAF1, we introduced five RAF1 mutants into NIH3T3 cells and examined ELK transactivation (Fig. 2D). ELK is a transcription factor, which is phosphorylated by activated ERK and then binds the serum response element in the promoter of the immediate-early genes, including *C-FOS*. ELK transactivation was enhanced in cells expressing p.S257L, p.N262K, and p.S427G without any stimulation, suggesting that these mutants were gain-of-function

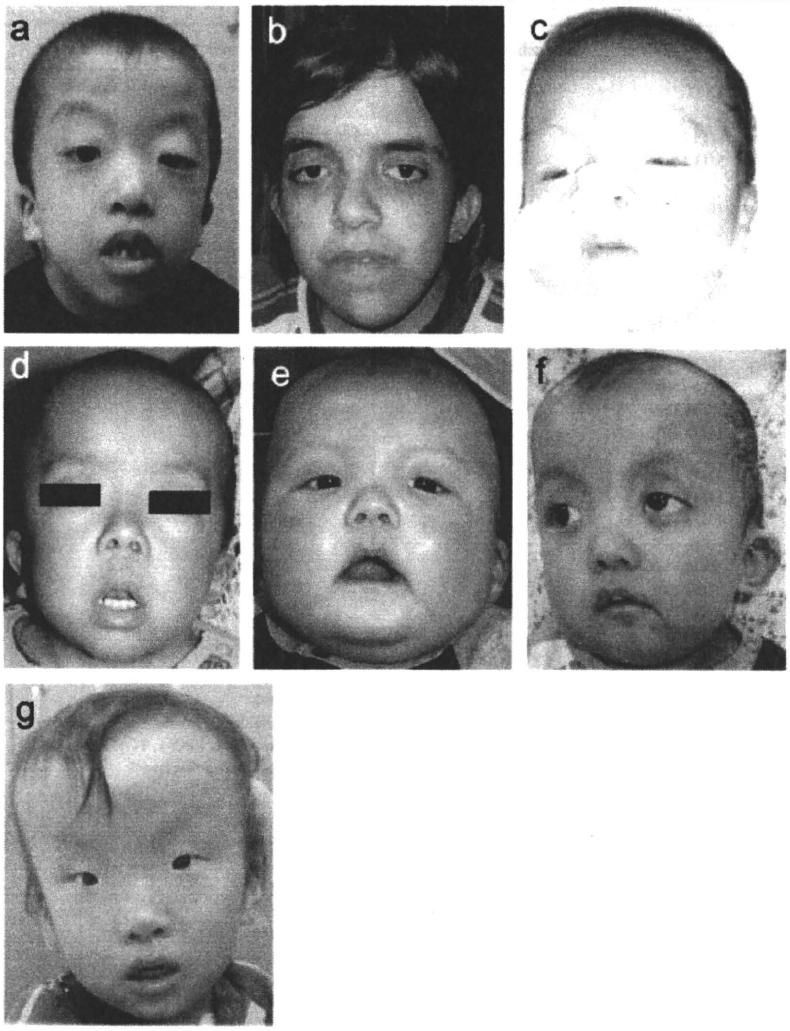

Figure 1. Facial appearance of patients with *RAF1* mutations. **a–f:** patients with p.S257L mutations. **a:** NS135; **b:** NS146; **c:** NS215; **d:** NS256; **e:** NS258 at 6 months; **f:** 2 years and 4 months; **g:** NS222 with p.S427G. [Color figure can be viewed in the online issue, which is available at www.interscience.wiley.com.]

mutations. ELK transactivation in cells expressing p.H103G and p.R191I was not enhanced.

Phosphorylation State, ERK Activation, and Binding to the Scaffolding Protein 14-3-3 in Mutations in the CR2 Domain

Previous studies as well as the present study showed that mutations in NS-associated *RAF1* mutations were clustered in the CR2 domain. We hypothesized that amino acid changes in the CR2 domain impaired phosphorylation of serine at 259. We additionally generated expression construct harboring p.S259F and p.P261A substitutions, and their phosphorylation status was examined using anti-pRAF1 (S259) antibody together with RAF1 WT, p.S257L, p.N262K, and p.S427G (Fig. 3A). The results showed that phosphorylated proteins were scarcely observed in p.S257L, p.S259F, p.P261A, and p.N262K. Phosphorylation of ERK p44/42 was determined using anti-p-ERK (p44/42) antibody. All mutations activated the downstream ERK without any stimulation. The level of ERK phosphorylation in cells expressing mutants was lower than that in those treated with epidermal growth factor (EGF), suggesting that the expression of p.S257L, p.S259F, p.P261A, and p.N262K resulted in a partial activation of ERK.

Anti-pRAF1 (S259) antibody was produced by immunizing rabbits with a synthetic phospho-peptide corresponding to residues surrounding Ser259 of human RAF1. To examine if this antibody was able to recognize phosphorylation at S259 when mutations such as S257L and N262K were introduced, we performed a solid-phase immunoassay using biotinylated peptides as per the manufacturer's recommendation (Mimotopes, Victoria, Australia; Supp. Methods). The result showed that at least in peptides, this antibody could recognize serine phosphorylation in amino acid 259 when mutations S257L and N262K were introduced (Fig. 3B). These results support the data in Figure 3A, suggesting that S259 was not phosphorylated in mutants in the CR2 domain.

To examine if the RAF1 mutants without S259 phosphorylation were able to bind to 14-3-3, we cotransfected three double mutants (WT/S621A, S257L/S621A, and N262K/S621A) with FLAG-tagged 14-3-3, and coimmunoprecipitation was performed using anti-Myc antibody (Fig. 3C). The result showed that the WT/S621A mutant bound 14-3-3. In contrast, p.S257L/S621A and

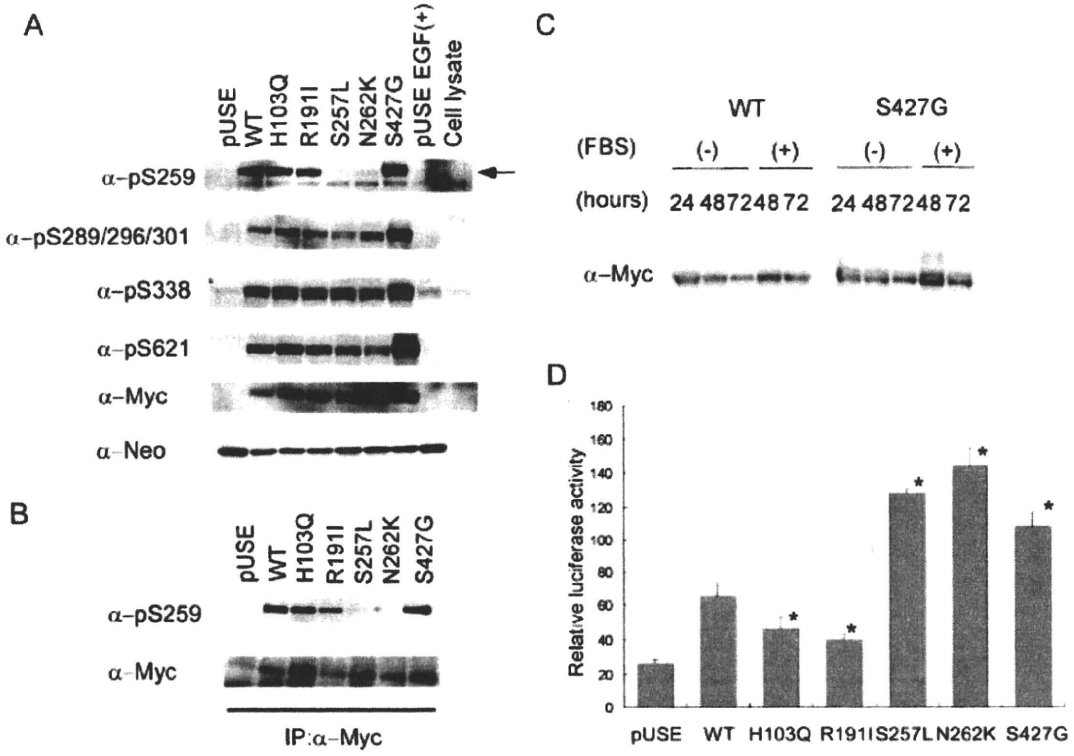

Figure 2. Analysis of phosphorylation status, degradation, and effect on downstream signaling in RAF1 mutants identified in this study. **A:** Phosphorylation status of wild-type (WT) RAF1 and mutants. Expression levels of RAF1 proteins and their phosphorylation levels were detected with different antibodies indicated in the figure. Transfection efficiency was measured using antineomycin phosphotransferase II (α-Neo) antibody. The arrow indicates the serine-phosphorylated expressed RAF1. **B:** Phosphorylation of S259 was confirmed by immunoprecipitation. Myc-tagged RAF1 was immunoprecipitated using anti-Myc antibody and the phosphorylation of S259 was determined. **C:** Time course experiments of WT RAF1 and p.S427G. The RAF1 protein was detected using anti-Myc antibody (clone 4A6; Millipore). FBS, fetal bovine serum. **D:** ELK transactivation in WT and mutants. Results are expressed as the means and standard deviations of mean values from triplicate samples. A significant increase in relative luciferase activity (RLA) was observed in cells transfected with p.S257L, p. N262K, and p.S427G, but not in cells transfected with p.H103Q or p.R191I. WT, wild-type; $^*P<0.01$ by Student's *t*-test.

p.N262K/S621A mutants did not bind 14-3-3, suggesting that the decreased phosphorylation of S259 prevented 14-3-3 binding. A similar result was obtained in the coimmunoprecipitation study using anti-FLAG antibody (Fig. 3D). These results showed that mutants in the CR2 domain impaired phosphorylation of S259, abrogated the binding to 14-3-3 and resulted in a partial activation of ERK.

Discussion

In this study, we identified eight different *RAF1* mutations in 18 patients: p.S257L in 11 patients and p.R191I, p.S259F, p.P261A, p.P261L, p.N262K, p.S427G, and p.L613V in one patient each. Sixteen patients were diagnosed as having NS, although we were not able to reevaluate 2 patients with Costello syndrome. Examination of detailed clinical manifestations in the present study and past studies showed that patients with *RAF1* mutations were associated with hypertrophic cardiomyopathy, arrhythmia, and mental retardation. Results from previous studies and the present study showed 41/52 (79%) mutations to be located in the CR2 domain (Fig. 3E). We first demonstrated that mutations in the CR2 domain had impaired phosphorylation of S259. This caused the impaired binding of RAF1 to 14-3-3, resulting in a partial activation of downstream ERK. These results suggest that dephosphorylation of S259 is the primary mechanism of activation of mutant RAF1 located in the CR2 domain.

Phosphorylation of S259 and subsequent binding to 14-3-3 have been shown to be important for suppression of RAF1 activity [Dhillon et al., 2007]. Light et al. [2002] examined the phosphorylation status at S259 in the p.S257L mutant. Their experiment showed that phosphorylation of S259 still existed in the p.S257L mutant. The mutant was not able to bind 14-3-3 [Light et al., 2002]. In contrast, our functional studies demonstrated that all four mutants located in the CR2 domain (p.S257L, p.S259F, p.P261A, and p.N262K) impaired phosphorylation of S259 and that two of them impaired binding of 14-3-3. Impaired binding to 14-3-3 was also shown in p.P261S mutant [Pandit et al., 2007]. The reason for the difference on S259 phosphorylation between the result by Light et al. [2002] and ours is unclear. Enhanced kinase activities of mutants, including p.S257L, p.P261S, p.P261A, and p.V263A, were demonstrated in a previous study [Razzaque et al., 2007]. Phosphorylation levels at S338 in p.S257L and p.N262K were not enhanced compared to that in WT RAF1 (Fig. 2A), suggesting that the activation mechanism in these mutants is different from that of the normal state upon RAS-GTP binding. Indeed, ERK activation was partial compared with that in cells after EGF treatment (Fig. 3A). These results suggest that the conformational change around S259 due to amino acid changes results in the decreased phosphorylation of S259 and that mutant

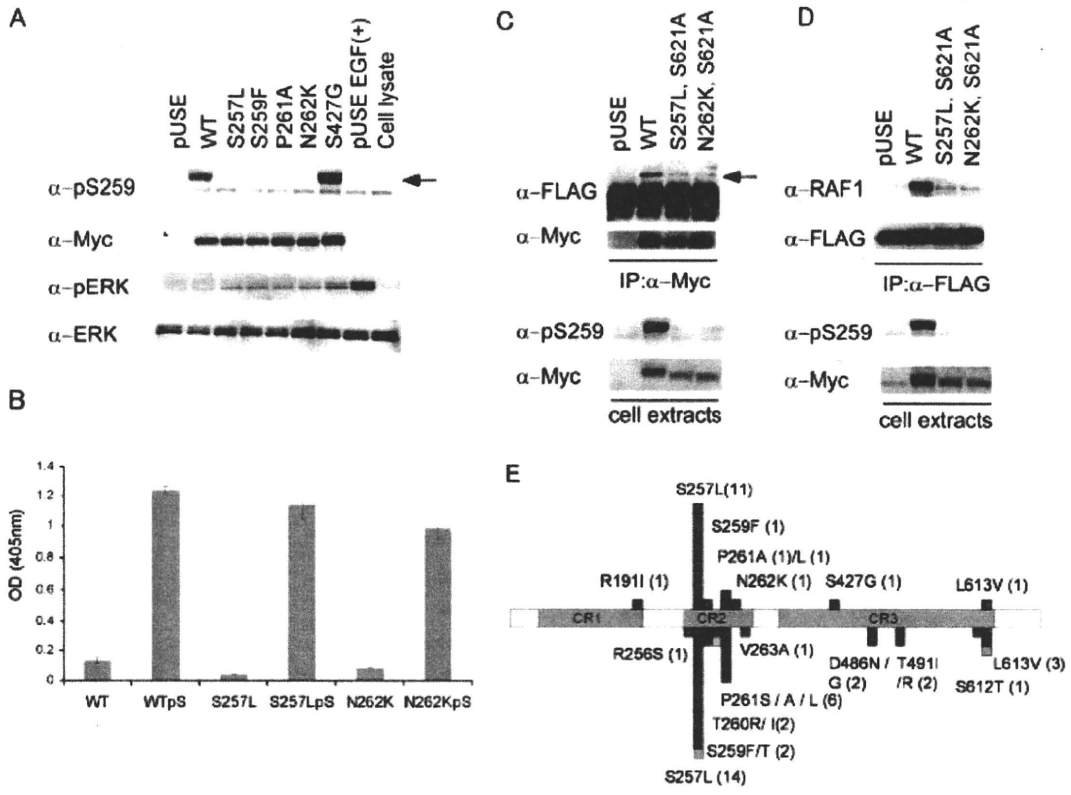

Figure 3. Phosphorylation of S259, binding to 14-3-3 and ERK activation of mutants located in the CR2 domain. **A:** Phosphorylation status of WT and mutants located in the CR2 domain. Phosphorylation of S259 was not observed in cells expressing p.S257L, p.S259F, p.P261A, and p.N262K. In order to examine the level of full activation of ERK, mock-transfected cells were treated with 10 ng/ml EGF. ERK activation was observed in cells expressing p.S257L, p.S259F, p.P261A, and p.N262K, but was weaker than those in cells expressing p.S427G and EGF-treated cells. The arrow indicates the serine-phosphorylated expressed RAF1. **B:** Epitope mapping of the anti-pRAF1 (S259) antibody using a solid-phase immunoassay. The antibody was able to recognize peptides with S257L or N262K mutations when S259 was phosphorylated, but was not able to recognize peptides without Ser259 phosphorylation. Results are expressed as the means and standard deviations of mean values from triplicate samples. **C:** Binding of RAF-1 to 14-3-3ζ. HEK293 cells were transfected with constructs harboring FLAG-tagged 14-3-3 and one construct of pUSE WT, p.S257L/p.S621A, or p.N262K/ p.S621A. Immunoprecipitation was performed using anti-Myc antibody, and 14-3-3 binding was determined by anti-FLAG antibody (upper panel). Phosphorylation of S259 and RAF1 expression were determined in cell lysates used for the immunoprecipitation (lower panel). The arrow indicates the band for 14-3-3. **D:** Binding of 14-3-3ζ to RAF-1. Immunoprecipitation was performed using anti-FLAG antibody and RAF1 binding was examined using anti-RAF1 antibody (upper panel). The binding of 14-3-3 to endogenous RAF1 was scarcely observed (lane 1, pUSE). Phosphorylation of S259 and RAF1 expression were determined using cell lysates used for the immunoprecipitation (lower panel). **E:** Domain organization and the distribution of mutations in RAF1 protein. The three regions conserved in all RAF proteins (conserved region [CR] 1, CR2, and CR3) are shown in pink. Mutations identified in this study are shown above the bar and those reported before [Ko et al. 2008; Pandit et al. 2007; Razzaque et al. 2007] are shown below the bar. Green squares indicate families with NS. Orange squares indicate patients with LEOPARD syndrome and the yellow square indicates a patient with hypertrophic cardiomyopathy.

RAF-1 then dissociates from 14-3-3; the substrate would thus be targeted to the catalytic domain in the CR3 domain (Fig. 4).

To highlight the clinical pictures of patients with *RAF1* mutations, clinical manifestations in 52 patients with *RAF1* mutations [Ko et al., 2008; Pandit et al., 2007; Razzaque et al., 2007], 172 patients with *PTPN11* mutations [Jongmans et al., 2005; Musante et al., 2003; Tartaglia et al., 2002; Zenker et al., 2004], 73 patients with *SOS1* mutations [Ferrero et al., 2008; Narumi et al., 2008; Roberts et al., 2007; Tartaglia et al., 2007; Zenker et al., 2007a] and 18 patients with *KRAS* mutations [Carta et al., 2006; Ko et al., 2008; Lo et al., 2008; Schubbert et al., 2006; Zenker et al., 2007b] are summarized in Table 3. The frequency of perinatal abnormalities was similar between patients with *RAF1* and *SOS1*. In contrast, the description of perinatal abnormalities was rare in patients with *PTPN11* and *KRAS* mutations. Growth failure and mental retardation were observed in 100 and 94% of NS with *KRAS* mutations, respectively. Growth failure and mental retardation were observed in 87 and 56% of patients with *RAF1* mutations, respectively. In contrast, those manifestations were less frequent (63 and 43%) in patients with *PTPN11* mutations. The frequency of mental retardation was lowest in patients with *SOS1* mutations (18%). We were unable to compare gene-specific features in craniofacial characteristics because such details were not described in the previous reports. As for skeletal characteristics, short stature was frequently manifested in patients with *RAF1* mutations (82%) followed by *KRAS* mutation-positive patients (71%). The association of short stature was lower in *PTPN11* mutation-positive and *SOS1* mutation-positive patients (56 and 38%, respectively). It is noteworthy that the association of hypertrophic cardiomyopathy was specifically high (73%) in *RAF1* mutation-positive patients. In contrast, hypertrophic cardiomyopathy was observed in 20% of clinically diagnosed Noonan

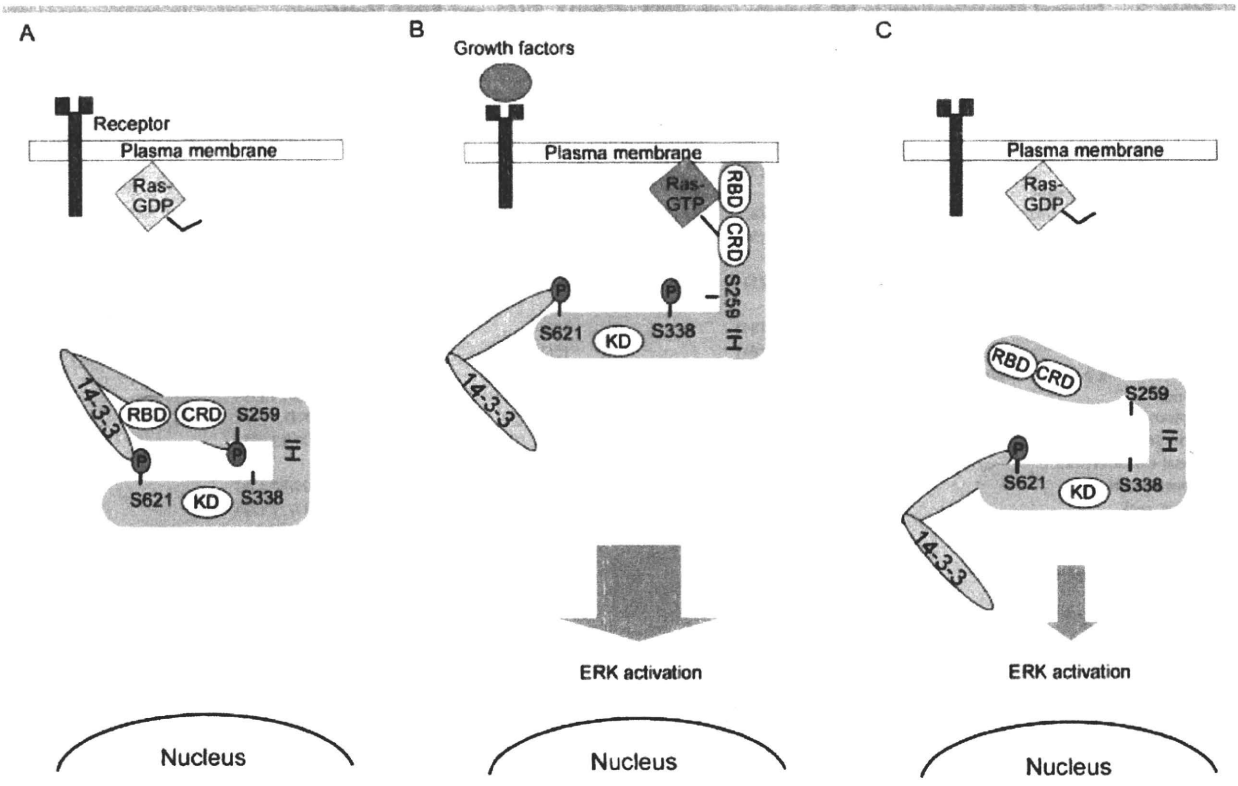

Figure 4. Schematic model of WT and mutant activation. **A:** In an inactive state, RAF1 is phosphorylated on S259 and S621 and is bound to 14-3-3. **B:** In growth-factor stimulation, the GTP-bound RAS binds to the CR1 domain of RAF1, which displaces 14-3-3. S259 is dephosphorylated by protein phosphatase 1 (PP1) and/or protein phosphatase 2A (PP2A). After RAF1 is recruited to the plasma membrane, phosphorylation of S338, Y341, T491, and S494 occurs. The phosphorylation of these residues is thought to be important for the full activation of RAF1. **C:** Mutants whose amino acid changes are located in the CR2 domain. It has been reported that S259 was phosphorylated by Akt and dephosphorylated by PP1 and/or PP2A. Amino acid changes in the CR2 domain would cause structural changes in the CR2 domain, leading to the access of PP2A to S259. Alternatively, Akt kinase would not be able to phosphorylate S259. S259 is dephosphorylated without stimulation and substrate(s) would be able to enter the kinase domain, leading to a partial activation. RBD, RAS-binding domain; CRD, cysteine-rich domain; KD, kinase domain; IH, isoform-specific hinge segment region. [Color figure can be viewed in the online issue, which is available at www.interscience.wiley.com.]

patients [van der Burgt 2007] and in 7, 10, and 17% of patients with *PTPN11*, *SOS1*, and *KRAS* mutations, respectively. These results strongly suggest that patients with *RAF1* mutations have a significantly higher risk of hypertrophic cardiomyopathy. Mitral valve abnormality and arrhythmia were also frequently observed in patients with *RAF1* mutations (27 and 56%, respectively). In summary, these results highlight specific manifestations of patients with *RAF1* mutations: high frequency of hypertrophic cardiomyopathy, septal defects of the heart, short stature, and less frequent PS (Supp. Fig. S1). The high frequency of heart defects would be associated with a high risk of sudden death in *RAF1* mutation-positive patients.

The present study is the first to identify p.S427G in a patient with NS. The same mutation has been reported in a patient with therapy-related acute myeloid leukemia [Zebisch et al., 2006]. The patient reported by Zebisch et al. [2006] first developed immature teratoma, yolk sack tumor, and embryonal testicular carcinoma. Thirty-five months after tumor resection and chemotherapy, the patient developed acute myeloid leukemia. Molecular analysis of *RAF1* revealed the de novo p.S427G mutation in leukemia cells and DNA from buccal epithelial cells [Zebisch et al., 2006]. Whether or not the patient had an NS phenotype was not mentioned. *RAF1* mutations have been rarely reported in malignant tumors. As far as we could determine, only six mutations, including p.P207S, p.V226I, p.Q335H, p.S427G, p.I448V, and p.E478K, have been identified in tumors and therapy-related leukemias [Pandit et al., 2007; Razzaque et al., 2007]. A previous study as well as our results showed that p.S427G mutant has transformation capacity [Zebisch et al., 2009], is resistant to apoptosis when introduced into NIH3T3 cells [Zebisch et al., 2009] and activates ERK and ELK transcription, suggesting that p.S427G is a gain-of-function mutation. We identified p.S427G in a familial case of NS. The mother and boy have not yet developed malignant tumors. Although no NS patients with *RAF1* mutations have developed malignant tumors, careful observation might be prudent in *RAF1* mutation-positive children.

We identified two novel mutations, p.R191I and p.N262K. p.R191I is located in the CR1, and arginine at amino acid position 191 is evolutionally conserved [Mercer and Pritchard, 2003]. Activation of ERK was not observed in cells expressing p.R191I. ELK transactivation was rather decreased; parental samples were not available. There is a possibility that this change is a polymorphism.

In conclusion, we identified *RAF1* mutations in 18 patients and detailed clinical manifestations in mutation-positive patients were examined. Our analysis of patients with mutations in *RAF1*, *PTPN11*, *SOS1*, and *KRAS* showed hypertrophic cardiomyopathy and short stature to be frequently observed in patients with *RAF1* mutations. Functional analysis revealed that dephosphorylation of S259 would be the essential mechanism for ERK activation in RAF1 mutations. Despite recent progress in molecular characterization of NS and related disorders, genetic causes in